Title
Comparison of free tropospheric western Pacific air mass classification schemes for the PEM-West A experiment

Journal
Journal of Geophysical Research Atmospheres, 101(D1)

ISSN
0148-0227

Authors
Smyth, S
Bradshaw, J
Sandholm, S
et al.

Publication Date
1996

DOI
10.1029/95JD02861

JOURNAL OF GEOPHYSICAL RESEARCH, VOL. 101, NO. D1, PAGES 1743–1762, JANUARY 20, 1996

Comparison of free tropospheric western Pacific air mass classification schemes for the PEM-West A experiment

S. Smyth,[1] J. Bradshaw,[1] S. Sandholm,[1] S. Liu,[2] S. McKeen,[2] G. Gregory,[3] B. Anderson,[3] R. Talbot,[4] D. Blake,[5] S. Rowland,[5] E. Browell,[3] M. Fenn,[6] J. Merrill,[7] S. Bachmeier,[8] G. Sachse,[3] J. Collins,[3] D. Thornton,[9] D. Davis,[1] and H. Singh[10]

Abstract. During September/October 1991, NASA's Global Tropospheric Experiment (GTE) conducted an airborne field measurement program (PEM-West A) in the troposphere over the western Pacific Ocean. In this paper we describe and use the relative abundance of the combustion products C_2H_2 and CO to classify air masses encountered during PEM-West A based on the degree that these tracers were processed by the combined effects of photochemical reactions and dynamical mixing (termed the degree of atmospheric processing). A large number of trace compounds (e.g., C_2H_6, C_3H_8, C_6H_6, NO_y, and O_3) are found to be well correlated with the degree of atmospheric processing that is reflected by changes in the ratio of C_2H_2/CO over the range of values from ~0.3 to 2.0 (parts per trillion volume) C_2H_2/ (parts per billion volume) CO. This C_2H_2/CO-based classification scheme is compared to model simulations and to two independent classification schemes based on air mass back-trajectory analyses and lidar profiles of O_3 and aerosols. In general, these schemes agree well, and in combination they suggest that the functional dependence that other observed species exhibit with respect to the C_2H_2/CO atmospheric processing scale can be used to study the origin, sources, and sinks of trace species and to derive several important findings. First, the degree of atmospheric processing is found to be dominated by dilution associated with atmospheric mixing, which is found to primarily occur through the vertical mixing of relatively recent emissions of surface layer trace species. Photochemical reactions play their major role by influencing the background concentrations of trace species that are entrained during the mixing (i.e., dilution) process. Second, a significant noncontinental source(s) of NO (and NO_x) in the free troposphere is evident. In particular, the enhanced NO mixing ratios that were observed in convected air masses are attributed to either emissions from lightning or the rapid recycling of NO_y compounds. Third, nonsoluble trace species emitted in the continental boundary layer, such as CO and hydrocarbons, are vertically transported to the upper troposphere as efficiently as they are to the midtroposphere. In addition, the mixing ratios of CO and hydrocarbons in the upper troposphere over the western Pacific may reflect a significant contribution from northern hemisphere land areas other than Asia. Finally, we believe that these results can be valuable for the quantitative evaluation of the vertical transport processes that are usually parameterized in models.

[1]School of Earth and Atmospheric Sciences, Georgia Institute of Technology, Atlanta.
[2]Aeronomy Laboratory, NOAA, Boulder, Colorado.
[3]NASA Langley Research Center, Hampton, Virginia.
[4]Institute for the Study of Earth, Oceans, and Space, University of New Hampshire, Durham.
[5]Department of Chemistry, University of California at Irvine, Irvine.
[6]Science Applications International Corporation, Hampton, Virginia.
[7]Center for Atmospheric Chemistry Studies, Graduate School of Oceanography, University of Rhode Island, Narragansett.
[8]Lockheed Engineering and Sciences Company, Hampton, Virginia.
[9]Department of Chemistry, Drexel University, Philadelphia, Pennsylvania.
[10]NASA Ames Research Center, Moffett Field, California.

Paper number 95JD02861.
0148-0227/96/95JD-02861$05.00

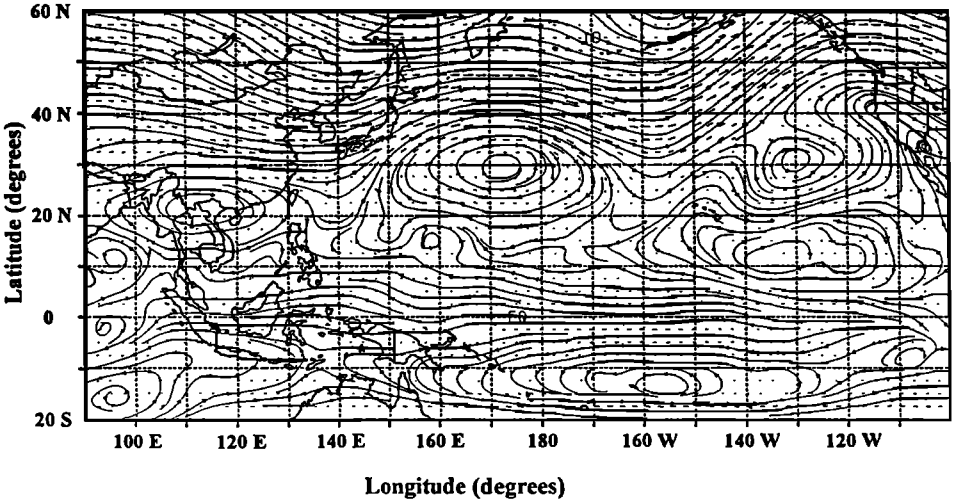

Figure 1. Mean 500-mbar nonmethane carbon (NMC) winds over the Pacific Ocean during PEM-West A with the following symbols.

1. Introduction

Long-range transport provides an effective means of exporting long lived carbon, sulfur, and nitrogen compounds from the northern hemisphere anthropogenic centers to the more remote Pacific. Chemical signatures in air over the western and eastern Pacific and, to a lesser extent, the central Pacific suggest this region is not immune to the effects of biogenic and anthropogenic emissions of relatively long lived compounds (i.e., lifetimes of days to months). Understanding the transportation and transformation processes affecting the abundances of nonmethane hydrocarbons (NMHCs), methane (CH_4), carbon monoxide (CO), carbon dioxide (CO_2), nitrogen oxides (NO_y), and ozone (O_3) is a key component in understanding the impact of biogenic and anthropogenic sources on the tropospheric chemistry within this region. During September and October 1991 the NASA Global Tropospheric Experiment (GTE) conducted a series of airborne Pacific Exploratory Missions over the western Pacific Ocean (PEM-West A). A complete overview of PEM-West A program goals and individual flight objectives and a description of the complete suite of instruments deployed to meet these objectives is given by *Hoell et al.* [this issue] and references therein. One major goal of the PEM-West A program was to accurately define the factors controlling the tropospheric budgets of carbon, nitrogen, sulfur, and ozone within this region. To this end we will use this unique data set to study the relative degrees to which atmospheric chemistry and dynamics are responsible for incorporating anthropogenically and biogenically perturbed air into the more pristine "background air" over the western Pacific.

During September and October 1991 the meteorology of the western Pacific played an important role in defining the distribution and variability of trace gases as outflow from the Asian continent was entrained into the air overlying the western and central Pacific. Meteorological conditions that affected the region during PEM-West A are discussed in detail by *Bachmeier et al.* [this issue] and *Merrill* [this issue]. The mean midtropospheric wind pattern for the PEM-West A study period is representative of the general flow patterns for the entire tropospheric column during the PEM-West A experiment [*Bachmeier et al.*, this issue; *Gregory et al.*, this issue] (depicted in Figure 1). The subtropical anticyclonic circulation in the central Pacific (located near 30°N and 160°E) was the most dominant feature affecting air originating from several locations. Flow from the Asian continent was mixed into the anticyclone along with air from the northern central Pacific and from the tropical/equatorial central Pacific. In the tropical western Pacific a small cyclonic circulation was apparent to the south-southwest of the subtropical anticyclone. This latter feature is a manifestation of several transient tropical cyclones, which often reached their maximum intensity over this particular region before recurving to the north and northeast. Air masses that had recently resided over China, India, Japan, Taiwan, and Indonesia represent the dominant short-range source of continental air affecting the western Pacific during this study. These air masses would be expected to exhibit different degrees of perturbation depending on the mechanism by which boundary layer air was transported into the free troposphere and the length of time the air resided within (or the degree it was mixed into) the general circulation patterns shown.

In companion papers, two methods are employed to classify air masses that were encountered in order to characterize their impact on the overall chemical state of the western Pacific. *Merrill's* [this issue] isentropic air mass back-trajectory analyses have been used to classify the chemical signatures of air masses having tropical versus extratropical marine origins [*Gregory et al.*, this issue] or continental origins [*Talbot et al.*, this issue]. In an alternative approach, *Browell et al.* [this issue] have classified air masses based on criteria developed from the lidar measurements of aerosols and ozone concentrations in order to investigate the fraction that various air mass categories contribute to the make up of the total tropospheric column over these regions. Our goal in this paper is to use a chemically based air mass segregation scheme and investi-

gate its ability to form a link between these other classification schemes and to provide a means of gaining additional insights into the factors that control the chemical composition over the western Pacific.

In this paper we will first examine in section 2 the chemical constitution of various air masses in relation to a scale that is defined by the relative abundance of the combustion products ethyne (C_2H_2) and CO. The relationship between this pair of compounds is then used in section 3 as a surrogate ordinate for examining the functional dependence of other trace gases relative to the degree that the atmosphere has processed emissions from combustion sources. These functional dependencies are examined in sections 4 and 5 for the relationships relative to air masses classified by isentropic back-trajectory and O_3/aerosol lidar analyses. The internal consistency between the chemically and trajectory-based schemes is tested in section 6 followed by a discussion of scientific issues that can be addressed by combining these three different air mass classification techniques.

2. Description of a Chemically Based Air Mass Classification Scheme

During PEM-West A number of trace gases (e.g., O_3, NMHCs, CH_4, CO, NO_x, and NO_y) that could serve as indicators of anthropogenic and biogenic emissions were found to be enhanced over the western Pacific with respect to air from the more remote central and southern Pacific [*Gregory et al.*, this issue; *Talbot et al.*, this issue]. In such instances where significant changes in trace gas levels occur between various air masses, corresponding changes in the relative abundances of NMHC compounds have been used as indicators of the relative "ages" of these differing air masses, especially when the compared compounds have common sources and different atmospheric chemical lifetimes [e.g., *Singh and Zimmerman*, 1992; *Parrish et al.*, 1992]. In a companion paper, *McKeen et al.* [this issue] discusses the anticipated and observed PEM-West A behavior of NMHC compounds and their relationships to one another as these compounds are mixed and photochemically degraded in the lower troposphere over the western Pacific. In particular, McKeen et al. once again demonstrate that the effects of mixing and photochemistry are often not distinguishable [e.g., *McKeen and Liu*, 1993], especially when they combine to process the compounds emitted into the atmosphere. In the lower troposphere during PEM-West A they find that this general conclusion holds for compounds that are less reactive with OH than normal butane (n-C_4H_{10}, with an OH lifetime of 3.2 days). Their study indicates that in the lower troposphere (<2 km), only the most reactive NMHC compounds (i.e., lifetime due to OH oxidation <1 day) have relative behaviors that were predictable based on photochemistry alone, whereas those with intermediate lifetimes (1-3 days) were controlled both by the photochemistry and dynamical processes (i.e., mixing) associated with advection, and those compounds with long lifetimes (>3 days) were primarily controlled by mixing. Their study also indicates that relationships between various compounds can be explored as markers of the relative degree that different air parcels have been impacted by the combined effects of different emission sources and differing combinations of photochemical and dynamical processing.

To explore the possibility of extending their work to the larger spatial scale of the western Pacific basin (defined here as the western tropical and northwestern midlatitude Pacific and adjacent continental regions), we will need to examine NMHC compounds that have atmospheric lifetimes longer than n-C_4H_{10}. Propane (C_3H_8) and ethane (C_2H_6) are both compounds with longer lifetimes that also have similar biogenic and anthropogenic sources and both undergo photochemical loss via H-atom abstraction when reacting with OH and as such are possible candidates for examining larger spatial scale atmospheric processes. Similarly, the combustion products C_2H_2 and CO represent a pair of compounds that have common primary anthropogenic sources and a common sink via loss due to O-atom addition upon reaction with OH. The reaction rates for these compounds vary somewhat as a function of temperature and pressure over the altitudes sampled during PEM-West A [*Demore et al.*, 1992]. The dependence on temperature is less for O-atom addition reactions than for H-atom abstraction reactions, but they (the O-atom addition reactions) are ternary reactions and therefore pressure dependent. However, these dependencies are modest for most tropospheric conditions ($< \pm 1.5$-fold from typical 500-mbar conditions). Based simply on the ratio of chemical lifetimes (i.e., $k_{2H2}/k_{CO} \sim 3$ and $k_{3H8}/k_{C2H6} \sim 5$), similar behaviors might be predicted as these pairs of compounds are photochemically processed following their input into the atmosphere. In this case, where atmospheric transport is ignored, a simple common photochemical processing timescale can be derived based on these compound reactions with OH, which can be expressed as

$$\Delta t = \ln(C_0/C_t)/k_c[OH] \quad (1)$$

where C_0 and C_t represent the concentration of the compound of interest at some initial time (0) and at some time later (t), and k_C is the compound's reaction rate coefficient with OH. This photochemical processing time concept can be extended in an attempt to remove the effects of simple dilution with pure air by using the relative behavior of two compounds with similar sources and sinks, where for the compounds C_2H_2 and CO,

$$\Delta t = [\ln((C_2H_2/CO)_0/(C_2H_2/CO))_t]/(k_{C_2H_2} - k_{CO})[OH]. \quad (2)$$

This pair of compounds has yielded useful information about the relative degrees to which different air masses have been processed within the atmosphere overlying remote regions [e.g., *Sandholm et al.*, 1992]. Over the western Pacific the mixing ratios of C_2H_6 and C_3H_8 were correlated with the observed ratio C_2H_2/CO (Figures 2a and 2b) as might be expected based on the relative photochemical processing time relationship described above. Even though these data display a high degree of correlation, there is a tendency toward nonlinearity at high and low values. The apparent plateau in C_2H_6 and C_3H_8 for mixing ratios of C_2H_2/CO larger than 1.5 (pptv/ppbv) is suggestive of the influence of variable source emission ratios of C_2H_6 and C_3H_8 relative to those of C_2H_2 and CO. The apparent plateau in mixing ratios below C_2H_2/CO values of about 0.5 (pptv/ppbv) suggests that some limiting value is reached that might represent the "background" mixing ratios for the

region. For C_2H_6 and C_3H_8 this lower limit would imply that the western Pacific background mixing ratios during the PEM-West A period were approximately 400 pptv and 18 pptv, respectively. The high degree of correlation that is displayed by the data in Figures 2a and 2b does suggest that common atmospheric processing mechanisms were operating on these compounds over the range of C_2H_2/CO ratios from about 0.5 to 1.5 pptv/ppbv. However, the above discussion also indicates that we must take into account that instead of simple dilution with pure air the mixing processes must involve dilution with air having nonzero concentrations of each compound (i.e., "background" mixing ratios≠0), in which case equation (2) no longer applies as a simple time marker (see also discussion of various cases described by *McKeen et al.* [this issue]).

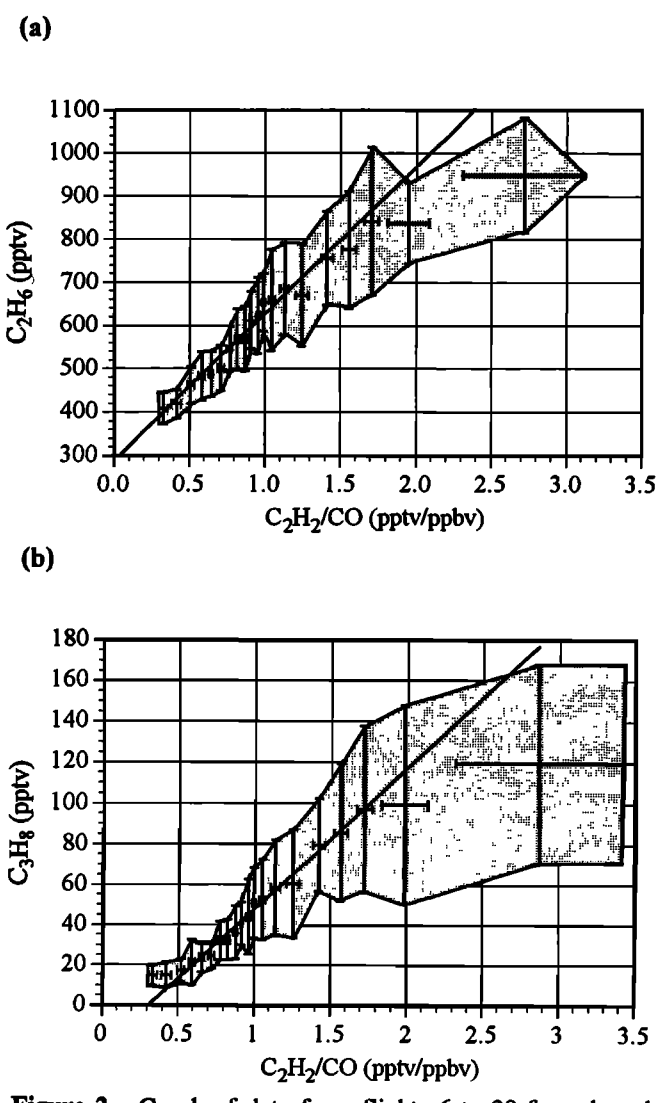

Figure 2. Graph of data from flights 6 to 20 for selected trace gases versus the ratio C_2H_2/CO, where error bars indicate $\pm 1\sigma$ about the mean for (a) C_2H_6 (r^2 = 0.96); (b) C_3H_8 (r^2 = 0.94); and where the least squares best fit line (thin line) is depicted for those data having associated C_2H_2/CO ratios between 0.5 and 1.5 pptv/ppbv. The shaded region represents the entire data set within $\pm 1\sigma$. These graphs include all of the PEM-West A nonmethane hydrocarbon (NMHC) data except the largest 1% of the mixing ratios which were omitted because they are believed to represent anomalously high mixing ratios measured in small spatial scale events from isolated emission sources. Each aggregate point in Figures 2a-2b contains 5% of the remaining 1084 NMHC measurements made during the portion of PEM-West A covering the western and central Pacific (flights 6-20) at altitudes higher than 2 km.

In the above discussion we have also ignored the in situ photochemical production of CO from CH_4 and NMHCs which has the same effect as reducing the rate constant for CO, (k_{CO}), in equation (2). In practice we can neglect the production of CO from reactive NMHCs, such as isoprene, which are oxidized in the continental boundary layer and cannot be distinguished from direct emissions of CO [e.g., *Altschuller,* 1991]. These effects are included in the observed initial value of C_2H_2/CO. Production of CO from less reactive NMHCs and CH_4 can be estimated from Figure 2 for each of the NMHCs [*Blake et al.*, this issue] and from model calculations [*McKeen et al.*, this issue]. These estimates indicate that in situ CO production has the same effect as reducing k_{CO} by about 20%.

To obtain some perspective for the relative magnitude to which mixing processes could contribute to the tendency displayed by the data in Figures 2a and 2b, we can use a somewhat overly simplified approximation that equates the effects of mixing in the western Pacific troposphere to dilution in a large exponential dilution flask. This coarse approximation allows us to roughly estimate an equivalent processing time due to mixing and dilution. In this simplistic case, an equivalent timescale due to dilution can be expressed by

$$\Delta t = \ln[(C_0 - C_d)/(C_t - C_d)]V/\mu \qquad (3)$$

where C_0 and C_t are the starting (C_0) and ending (C_t) concentrations in stirred volume V, and C_d is the concentration in the input flow having a volumetric flow rate μ [*Lovelock,* 1961]. Figures 3a and 3b depict qualitative representations of the relative contributions that might be expected from photochemical loss and the apparent loss due to mixing for the data presented in Figures 2a and 2b using a "starting" C_2H_2/CO ratio of 1.5 pptv/ppbv, which appears to approximate the beginning of the observed linear ln versus ln relationship that might be expected based on equations (1)-(3). For C_2H_2/CO values larger than 1.5 (pptv/ppbv) the curves is extrapolated from a C_2H_2/CO value of 1.5 (dashed portion). The line representing mixing is dashed after one 1/e-fold change (i.e., $\mu\Delta t/V$ = 1) and reflects dilution with air having the indicated background limited mixing ratios for each compound. For comparison the line representing photochemical loss is dashed after 10 days (i.e., after the approximate 1/e-fold time for the C_3H_8 reaction with a diurnally averaged free tropospheric OH concentration of 2.0 x 10^6 molecules cm^{-3} [*McKeen et al.*, this issue]). Thus the lines representing chemical loss and dilution by mixing are on different timescales but remain consistent on the relative scale determined by the C_2H_2/CO ratio.

From a reference frame standpoint we can also use the above coarse approximations to give a qualitative estimate of the timescale for mixing relative to photochemical loss. In this simplistic case we will use average circulation around the subtropical anticyclone requiring approximately 1 to 2 weeks [*Bachmeier et al.*, this issue; *Gregory et al.*, this

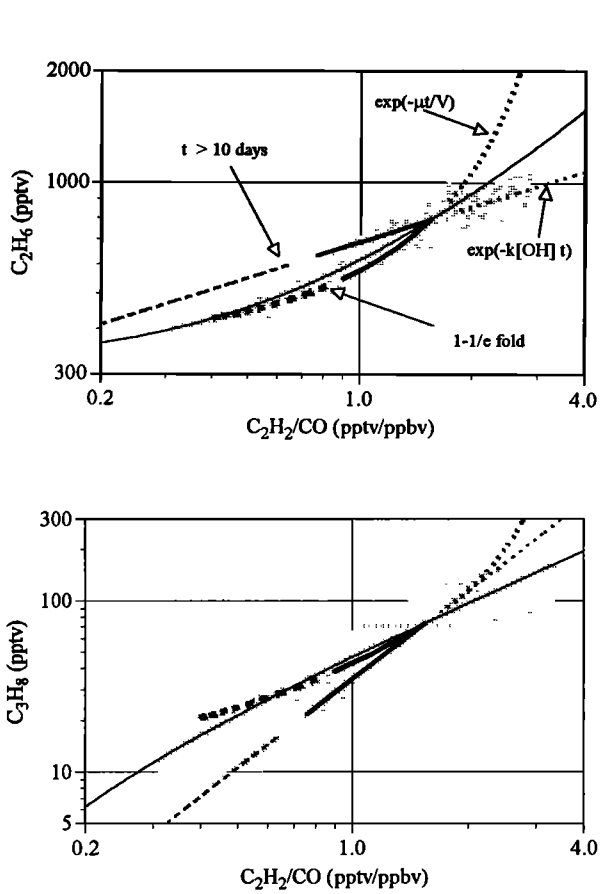

Figure 3. Representations of the relative effects of OH loss (thick line, dashed for t > 10 days and for C_2H_2/CO > 1.5) and mixing (thickest line, dashed after one-1/e-fold changes and for C_2H_2/CO > 1.5) with both starting at C_2H_2/CO values of 1.5 pptv/ppbv.

issue] and entrainment of continental air from Asia occurring primarily into the northern half of the anticyclone (μ=1.8x10^{14} m^3/s and V ~6x10^{14} m^3 for a 1-km-thick stable layer). From this we can estimate the effect of dilution alone with air having background limited mixing ratios (e.g., C_2H_2/CO ~0.3 pptv/ppbv). After 7 days of continental air (with C_2H_2/CO ~1.5 pptv/ppbv) flowing into the anticyclone (and a corresponding equal flow out), the expected C_2H_2/CO ratio would be approximately two-fold smaller than its initial value (i.e., 0.7 versus 1.5 pptv/ppbv). During the same 7 day period, reaction with a diurnal average OH concentration of 2.0 x 10^6 molecules cm^{-3} would result in a decrease of approximately 1.3-fold (i.e., 1.2 versus 1.5 pptv/ppbv) from photochemistry alone acting on the input flow. This 25% effect of photochemistry during the overall time the air mass is being atmospherically processed is in reasonable agreement with the 17% effect obtained from the model results of *McKeen et al.* [this issue]. Although these estimates give only a very rough approximation, three points are apparent. First, on this spatial scale of the western Pacific basin, mixing and chemistry may be expected to yield approximately the same magnitude of change for compounds with reactivities on the order of C_3H_8. This result for the western Pacific at large appears to extend the generality of the smaller spatial domain boundary layer work of *McKeen et al.* [this issue]. Second, the smallest observed C_2H_2/CO ratios (~0.3 pptv/ppbv) are well below expected values based on either mixing or chemistry alone acting on this processing timescale. Third, the C_2H_2/CO ratios observed during PEM-West A span a broad enough range of values (i.e., nearly an order of magnitude) to be useful as an ordinate for examining the functional dependence of other trace gases with respect to the chemical space defined by the ratio of C_2H_2/CO.

Based on the discussion above, it should also be apparent that the C_2H_2/CO-based air mass classification scheme is limited in its ability to distinguish between different combinations of conditions which could lead to the same apparent level of atmospheric processing. This ambiguity stems from the possibility that differing mixtures of continental air with different trace gas levels could be entrained into different "background air" under different meteorological conditions to yield similar levels of apparent atmospheric processing as expressed on the C_2H_2/CO scale. Even though this limitation will prevent the C_2H_2/CO-based scheme by itself from unambiguously identifying the sources impacting a particular air mass, it may provide a means by which perhaps otherwise chemically similar air masses may be coidentified and compared with respect to other tracer signatures.

3. Examination of Trace Gas Relationships With Respect to the C_2H_2/CO Ordinate

On the basis of the discussion above, the ratio of C_2H_2/CO appears to be a viable candidate for segregating air masses in relation to the relative degree to which they have been atmospherically processed and impacted by combustion sources. To assess this possibility, we selected several key compounds for analysis with respect to ratios of C_2H_2/CO; these are depicted in Figures 4a-4h. Measurements made in the boundary layer (or mixed layer) are omitted from this analysis, and data taken between 2- to 7-km are separated from those taken between 7- to 12-km. This altitude separation is based on the results of *Talbot et al.* [this issue] and *Gregory et al.* [this issue], which indicate that air of continental origin often had enhanced mixing ratios in the 4- to 8-km altitude regime.

The compounds CH_4, C_2H_6, and C_3H_8, which have both anthropogenic and biogenic sources, show an excellent correlation with respect to C_2H_2/CO. This tendency is also exhibited for the anthropogenically produced compound C_6H_6. Over the range of C_2H_2/CO values from 1.5 to 0.5 (pptv/ppbv), mixing ratios of CH_4 decrease from approximately 1745 to 1710 ppbv. This small relative change (i.e., 2%) is not unexpected for a compound that has a long tropospheric lifetime (~10 years). Also as expected, mixing ratios of the more reactive compound C_2H_6 (lifetime ~2 months) exhibit a greater decrease over this same range of C_2H_2/CO values, going from about 780 pptv to 460 pptv, and the even more reactive compounds (lifetimes of 1 to 3 weeks) C_3H_8 and C_6H_6 decrease by more than a factor of 3. For these compounds with primarily near-surface emission sources, there is also little difference in the observed mixing ratios between the 2- to 7-km and the 7- to 12-km altitude regimes when expressed against the C_2H_2/CO ordinate.

The above characteristics of hydrocarbons relative to C_2H_2/CO are expected because they and CO have a common

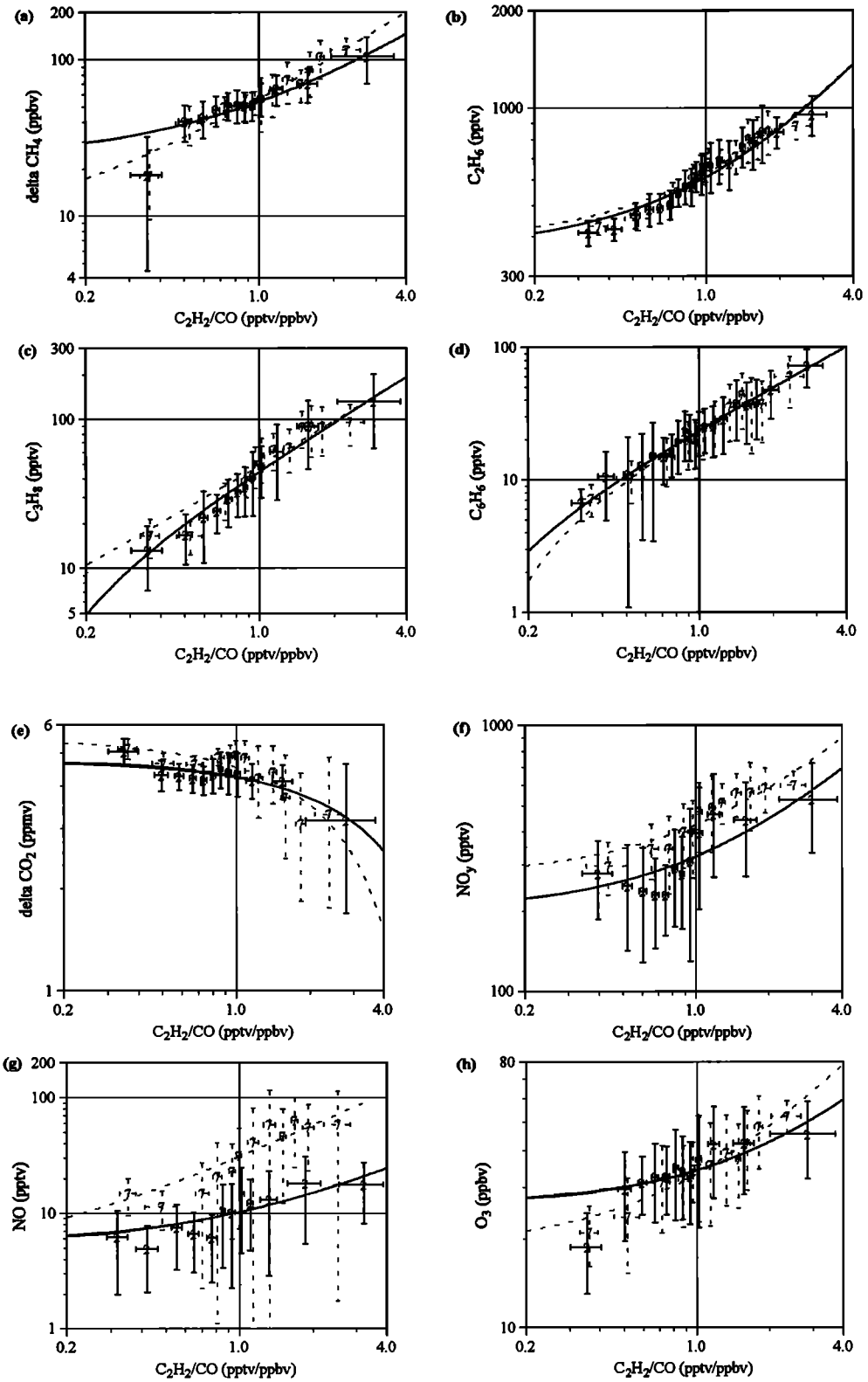

Figure 4. Graphs of the data similar to Figure 2 for flights 6 to 20 for selected trace gases versus the ratio C_2H_2/CO, separated into two altitude regimes (2 to 7 km (denoted by 2) and 7 to 12 km (denoted by 7), for (a) ΔCH_4 (2-7 km, r^2=0.96; 7-12 km, r^2=0.95); (b) C_2H_6 (2-7 km, r^2=0.96; 7-12 km, r^2=0.95); (c) C_3H_8 (2-7 km, r^2=0.98; 7-12 km, r^2=0.97); (d)C_6H_6 (2-7 km, r^2=0.92; 7-12 km, r^2=0.95); (e) ΔCO_2 (2-7 km, r^2=0.12; 7-12 km, r^2=0.5); (f) NO_y (2-7 km, r^2=0.81; 7-12 km, r^2=0.94); (g) NO_x (2-7 km, r^2=0-.91; 7-12 km, r^2=0.74); (h) O_3 (2-7 km, r^2=0.82; 7-12 km, r^2=0.78); and where NO_y and NO_x are for data taken using the Georgia Tech LIF instrument.

primary source in the continental boundary layer and share a common atmospheric sink due to OH reactions. Indeed, for all compounds depicted in Figures 4a-4d the overall lack of a statistically significant difference (outside $\pm 1\sigma$) between the data from different altitudes indicates that for these compounds the degree of atmospheric processing represented by the ratio of C_2H_2/CO is relatively independent of altitude. This tendency in the hydrocarbon compounds relative to C_2H_2/CO is partly due to atmospheric mixing or dilution by background air, and although atmospheric mixing itself is expected to be a purely physical process, the rate of dilution should also be proportional to the photochemical sink because mixing ratios of hydrocarbons in the background air are inversely proportional to their sinks. Thus Figures 4a-4d indicate that C_2H_2/CO is indeed a good measure for the degree of atmospheric processing.

Any trace species with a functional dependence or "trend" which deviates significantly from the trends of hydrocarbons discussed above would indicate different characteristics in its sources and/or sinks. As an example, even though the relationship is not so robust as others, ΔCO_2 mixing ratios do appear to reach a minimum in less processed air, a trend that could suggest biogenic CO_2 uptake dominates over CO_2 emissions from Asia (see also discussion by *Collins et al.* [this issue] and where the Δ refers to subtracting off the value of the smallest observed mixing ratio in order to accentuate trends in the data). This effect would produce a negative correlation between ΔCO_2 and C_2H_2/CO. On average, the largest values of CO_2 occur at the lowest values of C_2H_2/CO, which should represent air that is far removed from continental sources of C_2H_2 and CO or biogenic sinks of CO_2.

Unlike the hydrocarbon compounds, NO exhibits a significant positive altitudinal dependence with respect to its relationship to the C_2H_2/CO ratio (see Figure 4g). Some portion of this altitudinal dependence is due to the relatively rapid (i.e., timescale of minutes) photostationary state partitioning between NO and NO_2. The photochemical cycles controlling the partitioning between NO and NO_2 favors a larger fraction of NO at higher altitudes due to a slowing of the reaction rates forming NO_2 at higher altitudes (i.e., colder temperatures slowing the reaction $NO + O_3 \rightarrow NO_2 + O_2$; and smaller HO_2 concentrations slowing $NO + HO_2 \rightarrow NO_2 + OH$) in combination with enhanced NO_2 destruction rates [$J(NO_2)$] at higher altitudes. This would suggest that NO_x ($NO + NO_2$) should be a more conserved tracer than either NO or NO_2. *Davis et al.'s* [this issue] (GTE PEM-West A data archive) model-calculated "values" of NO_x ($NO_{x\ calculated} = NO_{measured} + NO_{2\ photostationary\ state\ calculated}$) yield little altitude dependence in the NO_x versus C_2H_2/CO relationship between the two altitude regimes shown in Figure 4g. However, measured values of NO_x exhibit an altitudinal tendency that is similar to that seen in NO. Several possible reasons exist for the difference between model-calculated and measured values of NO_2 (figures not shown here; see discussion by *Crawford et al.* [this issue]. Since all three parameters (i.e., $NO_{x\ measured}$, $NO_{x\ calculated}$, and $NO_{measured}$) exhibit overall similar tendencies with respect to C_2H_2/CO values (i.e., NO_x and NO values increasing with increases in C_2H_2/CO values) and the NO values have no similar current controversy about their validity, we will limit our discussion to solar zenith angle filtered NO values until these issues can be more fully resolved. Even so, our discussions will need to reflect anticipated changes with respect to the NO_x partitioning between NO and NO_2 as a function of temperature and ozone levels.

The trend in NO_y with respect to C_2H_2/CO also appears contrary to initial expectations. This is especially true if mixing ratios of NO_y, which represent the sum of the odd-nitrogen-containing compounds, are conserved as various forms of reactive odd nitrogen become chemically processed in the troposphere (e.g., $NO_x \leftrightarrow PAN$, $NO_x \leftrightarrow HO_2NO_2$, and $NO_x \leftrightarrow HNO_3$). Conservation of reactive nitrogen during transformations within the NO_y pool would suggest that NO_y mixing ratios should remain relatively constant as a function of changes in C_2H_2/CO ratios. In addition, the NO_y primary atmospheric sink, namely, the "irreversible" processes associated with rainout/washout (e.g., loss of HNO_3 and particulate NO_3) and dry deposition, has no direct relationship with the degree of atmospheric processing indicated by changes in the ratio of C_2H_2/CO. However, NO_y appears to follow the same magnitude of change in mixing ratios with respect to C_2H_2/CO values as that exhibited by the moderately long lived compound C_2H_6. This similarity between NO_y and C_2H_6 and their relationship with respect to the C_2H_2/CO ordinate could be due to the NO_y heterogeneous removal being proportional to the ratio of HNO_3 and NO_y which, in turn, is proportional to the concentration of OH. Furthermore, since the probability that heterogeneous removal has occurred tends to increase with time, it should also increase with the degree of atmospheric processing. On the other hand, the implied long lifetime of NO_y (about 2 months) seems to suggest either a very inefficient or even reversible heterogeneous removal process or the occurrence of significant in situ NO_y source(s) in the free troposphere. This is demonstrated more clearly in Figures 5a and 5b which show that the ratio NO_y/O_3 exhibits little change with respect to changing values of the ratio C_2H_2/CO, while the ratio C_3H_8/C_2H_6, which does not have in situ sources, depicts a clear trend. Some portion of this implied long-lifetime behavior may also be due to contributions from compounds such as HCN and possibly other nonoxides of nitrogen that are a part of the NO_y measurements presented here [*Sandholm et al.*, 1994].

The above relationships may also help explain the significant correlations between the average mixing ratios of NO_y and O_3 that have now been observed in several remote tropospheric data sets [e.g., *Hübler et al.*, 1992; *Sandholm et al.*, 1994]. Since O_3 is essentially inert (i.e., production approximately equal to loss) in the upper troposphere, the trends displayed in Figure 5a suggest that the NO_y lifetime must be either equally long or there is a widely distributed NO_y source(s) which is of the same order of the NO_y sink (i.e., NO_y production is also approximately equal to NO_y loss). This would lead to little change in the average relationship as a function of the degree of atmospheric processing (i.e., NO_y/O_3 ratio is relatively constant versus the C_2H_2/CO ordinate; see Figure 5a).

To fully distinguish between the causes of the tracer relationships discussed above, additional information about the various air masses history is needed as the C_2H_2/CO ordinate alone cannot identify what type of air mass has been processed (or modified) or in what way. In principle, meteorologically based classification schemes could compliment the segregation obtained from the chemically based atmospheric processing scale.

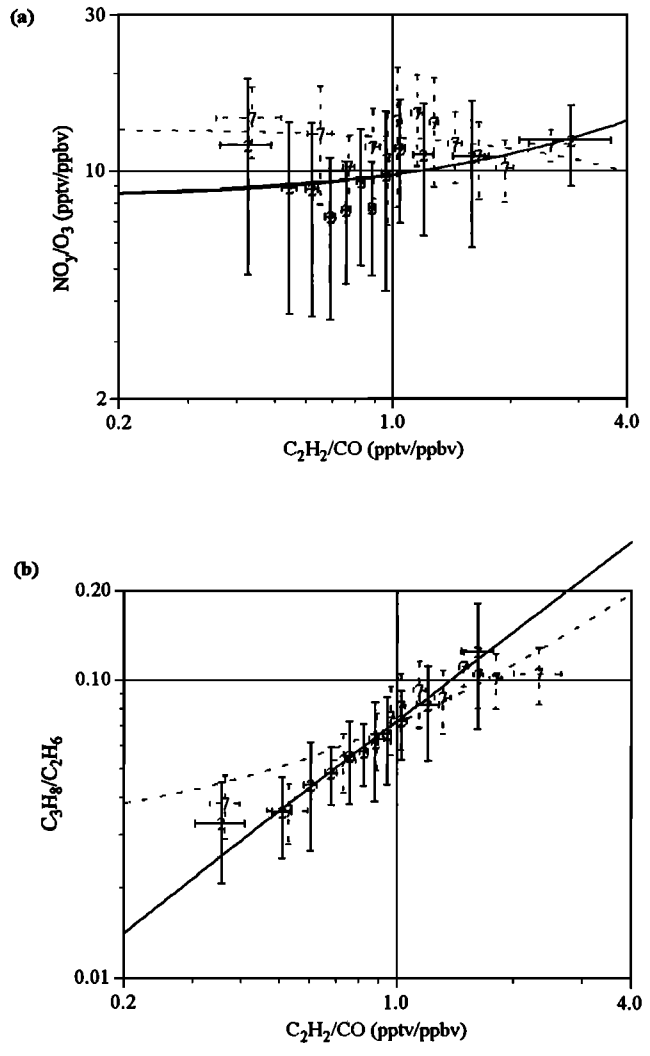

Figure 5. Graphs depicting the effects of atmospheric processing for (a) NO_y/O_3 (2-7 km, $r^2=0.49$; 7-12 km, $r^2=0.1$); and (b) C_3H_8/C_2H_6 (2-7 km, $r^2=0.99$; 7-12 km, $r^2=0.95$).

4. Comparison to Trajectory-Based Continental and Marine Air Mass Classification Schemes

In companion papers, *Talbot et al.* [this issue] and *Gregory et al.* [this issue] present analyses of the chemical composition and chemical signatures found in air masses defined as having continental and marine origins based on the isentropic back-trajectory analyses of *Merrill* [this issue]. Table 1 gives a listing of the classification schemes adopted in these studies, which can be broken into the general air mass origin regions depicted in Figure 6. The chemical characteristics of air masses classified by Gregory et al. and Talbot et al. are depicted in Figures 7a-7h with respect to the degree of atmospheric processing indicated by the ratio of C_2H_2/CO. Gregory et al's. northern (N) marine and southern (S) marine classification scheme restricted trajectories to greater than 10 days over the Pacific and excluded all cases where inspection revealed that trajectories could have been directly modified by continental outflow as indicated by a trajectory approach to within approximately 500 km of the Pacific rim. As might be expected based on the data segregation along the C_2H_2/CO ordinate, the average chemical composition of the northern (N) marine air masses was found to differ significantly from those of the southern (S) marine classifications [*Gregory et al.*, this issue]. For the greater than 10-day-old northern marine air masses, the tracers NMHCs, ΔCH_4, NO_y, and O_3 span a wide range of C_2H_2/CO values going from approximately 0.6 to 1.8 pptv/ppbv. This suggests that these trace gases continue to vary coherently with the degree of atmospheric processing represented over this range of C_2H_2/CO ratios in these greater than 10-day-old air masses. A similar argument can be made for the southern marine air masses that are associated with what should have been relatively pristine air of equatorial Pacific origin. On average, these latter air masses do exhibit the smallest trace gas mixing ratios (with the exception of CO_2) and values of the C_2H_2/CO ratio of those observed during PEM-WA.

For comparison the continental outflow data classified by *Talbot et al.* [this issue] are also depicted in Figures 7a-7h, for their northern continental (originating over China and

Table 1. Large-Scale Trajectory Analysis Based on Air Mass Classification Schemes

Article	Case Study	Origin	Type	Code
Gregory et al. [this issue]	northern marine	> 10°N latitude	marine (> 10 days)	N
	southern marine	< 10°N latitude	marine (> 10 days)	S
Talbot et al. [this issue]	southern continental	< 30°N latitude	continental (≤ 2 days)	I
	southern continental	< 30°N latitude	continental (2-4 days)	i
	northern continental	> 30°N latitude	continental (≤ 2 days)	C
	northern continental	> 30°N latitude	continental (2-4 days)	c

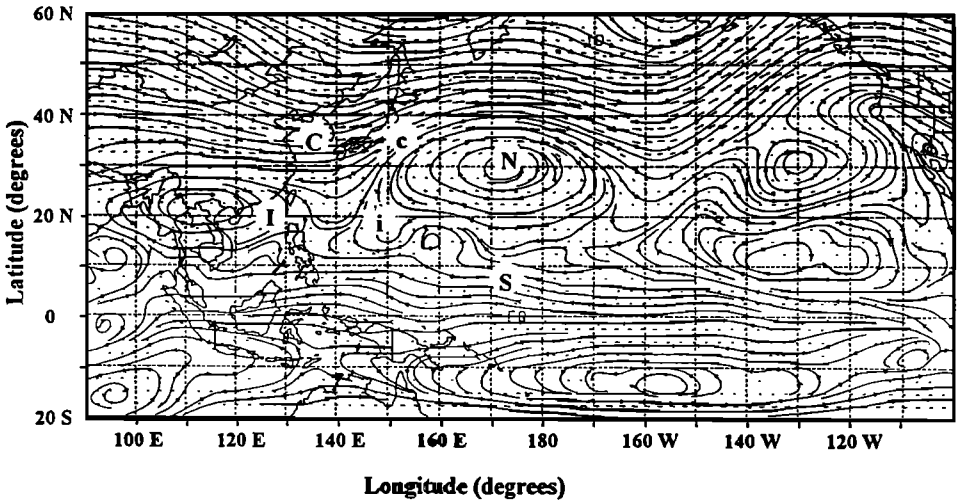

Figure 6. Representation of typical regions of well-defined air mass origins superimposed on the NMC 500-mbar mean wind pattern, where central Pacific is (A), equatorial Pacific (Q), tropical western Pacific (T), and modified western Pacific (M).

Japan, designated C and c) and southern continental (originating from over India and southeast Asia, designated I and i) classifications. These cases were taken, based on an inspection of the trajectories, to characterize the general outflow patterns encountered by the aircraft and where the upper and lower case designations separate less than 2-day from 2- to 4-day air mass travel times from land. The air masses originating from the northern continental regions (C and c) have on average larger trace gas mixing ratios than those originating from the southern continental regions (I and i). In both cases the air masses that were encountered within approximately 2 days or less from land (C and I) had trace gas mixing ratios that were only slightly larger (~1.5-fold) than values found in what could be considered the "chemically youngest" (i.e., larger C_2H_2/CO values) northern marine air masses (N) that had travel times of at least 10 days from land sources. This similarity seemingly indicates that within about 2 days, continental air masses appear to blend in with the chemical signatures found in the circulation patterns over the western Pacific and suggests atmospheric processing can efficiently and perhaps quickly reduce trace gas mixing ratios toward the average values found in the work of Gregory et al.'s northern marine air mass classifications. Perhaps contrary to initial expectations, the more moderately aged continental classifications (c and i) have quite different chemical signatures, which appear to reflect some impact from anthropogenic inputs in one case (c) and more "aged" marine air in the other (i). In all of these cases, use of the C_2H_2/CO ordinate as a "chemically based" air mass classification scheme appears to compliment the trajectory-based scheme by providing a means to further delineate air masses within an otherwise similar coarse scale dynamical framework (e.g., "aged" marine air or continental air).

5. Comparison to Lidar O_3 and Aerosol-Based Air Mass Classification Scheme

Browell et al. [this issue] have also classified PEM-West A air masses using their range-resolved lidar measurements of aerosol and O_3. These tropospheric column measurements, in conjunction with potential vorticity cross sections (to help define stratospherically influenced air), were used to set discriminator levels that distinguish between different air masses. A summary of the air mass classification types defined by Browell et al. is given in Table 2. In some instances, more complete chemical characterization in situ sampling was also performed in the same air profiled by the lidar instrument, making possible comparison of tracer signatures between the lidar-based and chemically based (i.e., C_2H_2/CO ratio based) schemes. Figures 8a-8h compare the results from those lidar-based air mass classifications that were in situ sampled versus the entire data set segregated on the C_2H_2/CO ordinate.

In their work the lidar-based scheme classified approximately 1/3 of the western Pacific upper troposphere column as having been stratospherically influenced (designated by F in Figure 8) for latitudes greater than approximately 20°N, whereas little, if any, stratospheric influence was observable below approximately 6 km. They also concluded that these stratospherically influenced air masses generally subsided as they traveled around the subtropical anticyclone, and therefore they should have eventually influenced the lower troposphere of the central Pacific and thus the "background air" of the Pacific basin's lower troposphere. On average, the chemical composition found in the stratospherically influenced classification (F) supports the lidar-based designation. For example, O_3 and NO_y mixing ratios are at the upper end of the range for this C_2H_2/CO grouping as might be expected for air enriched by stratospheric inputs of O_3 and NO_y [*Murphy et al.*, 1993].

They also identified plumes with enhanced aerosol loading, which were primarily found in the lower 6 km and were more frequently found in the midlatitudes (approximately 1/2 of the air masses they classified as plumes over the range of 20° to 40°N, designated by H, L, and B in Figure 8b). In contrast, aerosol-enhanced air masses in the upper troposphere were primarily identified as originating from continental and marine convective outflows (designated by C and O). In the tropics, approximately 80 to 90% of the upper tropospheric air masses were classified as having been impacted by convective outflows. The remainder of

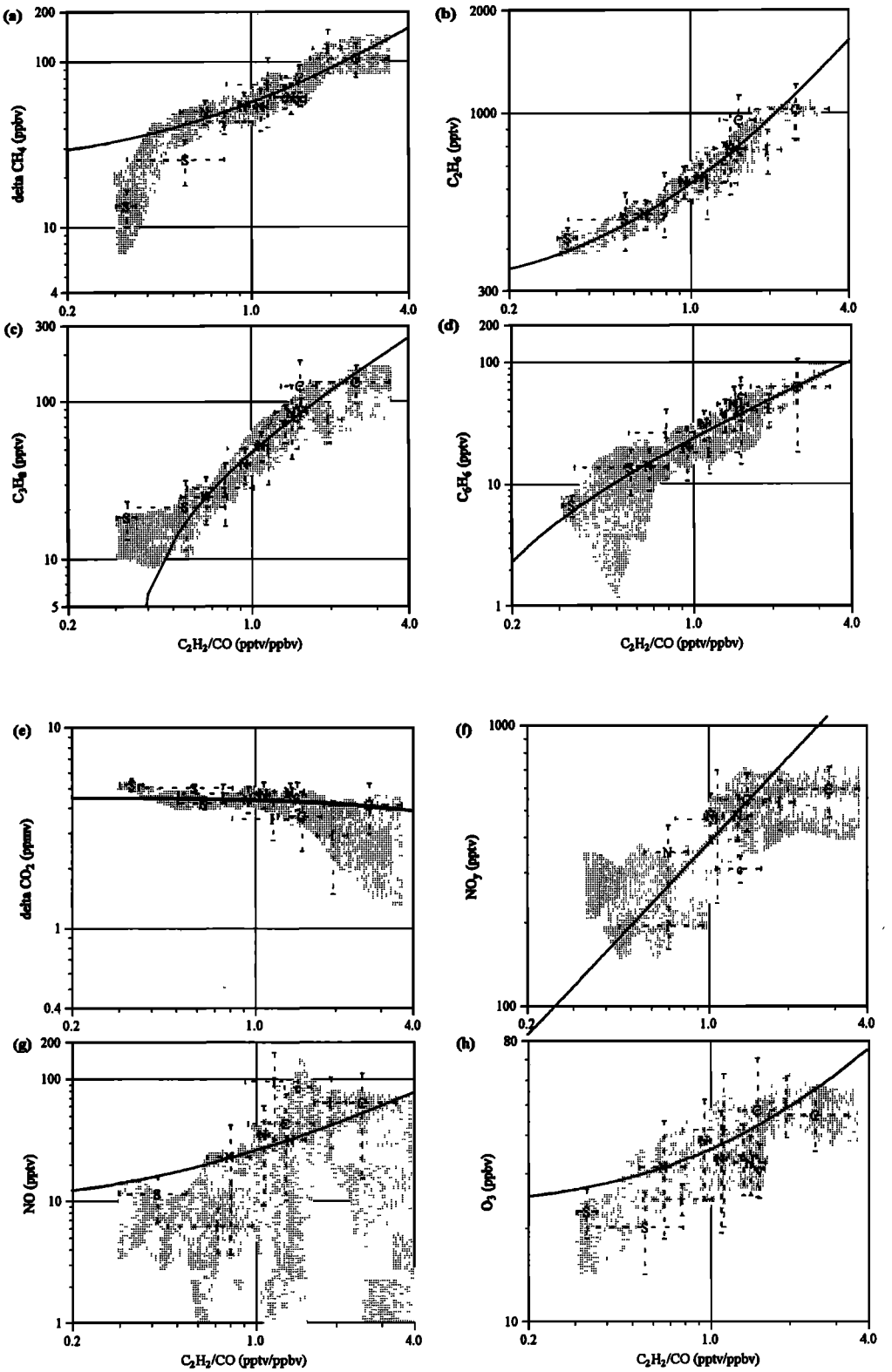

Figure 7. Relationships between the degree of atmospheric processing indicated by the ratio C_2H_2/CO and large-scale trajectory-based air mass classification schemes of *Gregory et al.* [this issue] and *Talbot et al.* [this issue] for northern marine (N), southern marine (S), southern continental less than 2-day (C), southern continental from 2- to 4-day (c), northern continental less than 2-day (I), and northern continental from 2- to 4-day (i) types of air masses.

Table 2. Lidar O_3 and Aerosol-Based Air Mass Classification Schemes

Article	Case Study	Origin	Type	Legend
Browell et al. [this issue]	stratosphere-influenced air	upper troposphere	stratosphere	F
	high-ozone plume	possibly mixed	suspected continental	H
	low-ozone plume	possibly mixed	suspected marine	L
	background plume	possibly mixed	suspected continental influence	B
	background air	possibly mixed	suspected marine	K
	clean Pacific air	remote Pacific	marine	P
	convective outflow	possibly mixed	suspected marine	O
	continental convective outflow	North and South Asia	suspected continental	C

the nonstratospheric or nonplume air masses were classified as predominately background (designated by K) or clean Pacific (designated by P).

Of the various air masses classified as plumes, those classified as high-ozone plumes (H) would be expected to exhibit the effects of enhanced rates of O_3 producing reactions if these air masses had NMHCs and reactive nitrogen mixing ratios that are typical of the range found in western Pacific continental outflows [*Liu et al.*, this issue; *Davis et al.*, this issue]. These lidar-classified air masses do have NO_y and NMHCs mixing ratios that are of the order of those observed in continental outflows that were less than 2 days travel time from the Asian continent (compare Figures 7 and 8) indicating that their chemical compositions are consistent with what might be expected for air that had been impacted by anthropogenic sources.

The air that they classified as having been convectively pumped into the western Pacific troposphere is seen to generally fall into the two distinct categories identified by the lidar-based groupings. The air characterized as continental convective outflow (C) has mixing ratios that are consistent with those found in the trajectory-based classification of continental air masses. In particular, mixing ratios of most compounds are similar to those found in the northern continental 2- to 4-day and the southern continental < 2-day classifications. Similarly, the convective outflow classification (O) also follows our expectations for air masses influenced by convection over the marine environment. On average, NMHC mixing ratios for this classification are near the smallest values for this C_2H_2/CO range, whereas NO_y mixing ratios are enhanced. This follows the trend that might be expected based on convection of relatively clean marine boundary layer air [*Gregory et al.*, this issue] coupled with the production of NO_x by lightning.

The air classified as low-ozone plume (L), clean Pacific air (P), background (K), and background plume (B) all fall within the center of the C_2H_2/CO ratio-based groupings of the data. These lidar-classified air masses have similar chemical relationships as the trajectory-based continental south 2- to 4-day (c) and north marine (N) classifications of air masses. The chemical signature of the low-ozone plume (L) classification lies in the middle of the distribution for the entire data set, whereas the clean Pacific air classification (P) appears closer to air originating from the equatorial regions characterized in the south marine classification.

On average, the mixing ratios of NMHCs, CO_2, and NO_y in the background plume classification (B) are at the upper end of the range for this C_2H_2/CO grouping of data suggesting that the lidar-based plume designation may be correctly indicating a partial continental influence. Isentropic back trajectories indicate that this low-altitude (~2km) background plume subset of data originated from the region classified as the tropical western Pacific. The plume designation in conjunction with enhanced NMHC mixing ratios and a relatively low O_3 and CH_4 mixing ratios are indicative of what would be expected for otherwise clean marine air that had been modified by aged biomass burning (i.e., low NO_x/NO_y ratio), which was occurring in Indonesia during the time of the PEM-West A experiments.

On the basis of the discussions above, there does appear to be some commonality between the air masses classified by the chemically and lidar-based schemes. However, unlike the trajectory-based scheme, the lidar-classified air masses tend to overlap significantly along the C_2H_2/CO ordinate. Thus the lidar-based scheme, which primarily classifies air

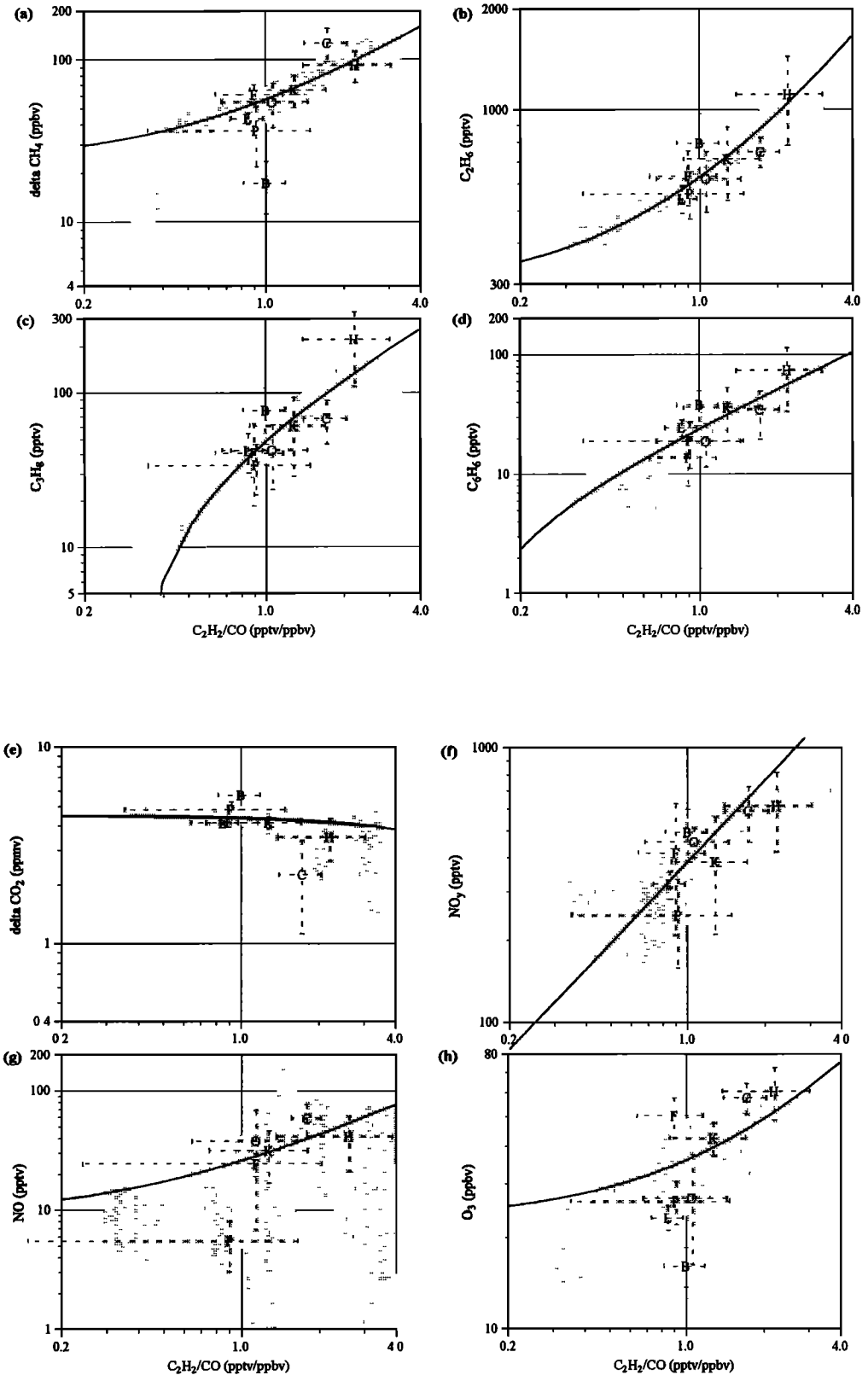

Figure 8. Relationships between the degree of atmospheric processing indicated by the ratio C_2H_2/CO and the O_3 and aerosol-based air mass classification scheme of *Browell et al.* [this issue], for high-ozone plume (H), low-ozone plume (L), convective outflow (O), continental convective outflow (C), background plume (B), and background (K), clean Pacific (P), and stratospherically influenced (F) types of air masses.

masses by the levels of O_3 and aerosols, tends to give air mass groupings that have a similar degree of atmospheric processing with respect to the surface source combustion tracers C_2H_2 and CO. This is not surprising because the lidar-based scheme is not designed to use the continent as the reference point. Furthermore, the overlap may be due to the fact that sinks of O_3 and aerosols are rather different from those of C_2H_2 and CO. In addition, there are other significant sources of O_3 and aerosols than those in the continental boundary layer. Nevertheless, this comparison suggests that the lidar-based scheme identification of those air masses that were substantially influenced by continental outflow of trace species (H and C in Figures 10a-10h) is consistent with expectations from the other schemes. In addition, this comparison agrees, in general, with the lidar-based scheme's identification of those air masses that were influenced by stratospheric intrusions (F in Figures 10a-10h).

6. Evaluation of the Consistency of Trajectory and Chemically Based Schemes

In contrast to the lidar-based scheme the air masses classified by the trajectory-based scheme are well segregated in the chemical space or coordinate system (i.e., C_2H_2/CO) provided by the chemically based atmospheric processing scheme. The consistency displayed between these latter two schemes is not surprising if one recalls that the chemically based scheme is designed to provide a measure of the degree of total atmospheric processing experienced by an air mass starting from the moment C_2H_2, CO, and other trace species are emitted. This design should be well matched by the trajectory-based scheme, which takes the Asian continent and the Pacific rim countries as the reference point for an air mass origin. A valuable test of the consistency between the chemically based scheme for classifying air masses and the trajectory-based scheme is to compare the air mass travel time from land derived from the latter with the degree of atmospheric processing from the former. To do this, we need to express the degree of atmospheric processing, including photochemical reactions and mixing in an equivalent pseudo-OH reaction time as defined in equation (2) for C_2H_2/CO (denoted process time herein after). This process time places all factors that affect the degree of atmospheric processing on the time coordinate of the OH reaction with C_2H_2 and CO (i.e., the corresponding time for reaction with OH to remove an equivalent amount of the compound). In equation (2), reaction rate constants at 500 mbar are used, i.e., 6.0×10^{-13} cm^3/s for k_{C2H2} and 1.95×10^{-13} cm^3/s for k_{CO} [*Demore et al.*, 1992]. Furthermore, k_{CO} is reduced by 20% to account for the production of CO from NMHCs and CH_4 as discussed earlier.

The first step of the test is to show that the travel time from land and the process time of various air masses are of the same order. From our earlier discussion it is obvious that both schemes give shorter times for continental air masses than for marine air masses. This is also true on a finer scale; for example, the continental air masses with shorter travel times from land (I and C in Table 1 and Figures 7a-7h) also have shorter process times than those of the continental air masses with longer travel times (i and c in Table 1 and Figures 7a-7h).

It is interesting to note that the sequence of the process time depends also on the latitude of the origin of the air mass, as indicated by the fact that air masses at higher latitudes tend to have shorter process times (or less atmospheric processing). Assuming a constant C_2H_2/CO value in the emissions, there are two likely factors that would contribute to this phenomenon. One is that the atmospheric sink is smaller at higher latitudes due to smaller OH concentrations. It is also possible that air masses at lower latitudes tend to go through greater convective mixing or dilution resulting in longer process times (or more atmospheric processing).

The second step of the test is to compare the values of travel time from land to the indicated process time. Since the process time includes the equivalent amount of OH reaction "time" due to dilution (denoted dilution time herein after), it is expected to be greater than the travel time and the difference between them is a measure of the degree of dilution. From Table 1 it can be seen that the travel times from land are relatively well defined for the northern continental 2- to 4-day (c) and southern continental 2- to 4-day (i) classified air masses. So these air masses have been selected first for the second step of the test. The corresponding median values of C_2H_2/CO for these air masses in Figures 7a-7h range from 0.8(i) to 1.6(c) pptv/ppbv. Assuming an initial emission C_2H_2/CO value of 8.7 pptv/ppbv and a spatial and temporal average OH concentration of 2×10^6 cm^{-3} [*Blake et al.*, this issue; *McKeen et al.*, this issue], equation (2) yields process time values ranging from 22 to 31 days. Thus the corresponding dilution time should range from 18 to 29 days which is about 8 times greater than the average travel time from land. A similar conclusion can be made for other air masses classified in Table 1 when their process times and dilution times are calculated starting from the time of emissions. Although we fully expect the process time to be greater than the travel time from land, the predominant fractional contribution of the dilution time to the overall process time is surprising.

Uncertainties involved in the above estimate come primarily from the initial emission ratio of C_2H_2/CO and model-calculated OH concentration. The former is derived from several flights into major urban emissions [*Blake et al.*, this issue]. If the emission ratio of 8.7 pptv/ppbv is too high, it would lead to an overestimate of the process time and the dilution time. However, from Figures 7a-7d the minimum value for the initial emission ratio of C_2H_2/CO has to be about 4. This value would yield process time values ranging from 12 to 21 days, still much longer than the travel time from land. In addition, as will be discussed below, model calculation [*McKeen et al.*,this issue] with the emission ratio of 8.7 pptv/ppbv yields results similar to those of Figures 7a-7d, suggesting that the emission ratio is not too large. A larger OH concentration would reduce linearly the calculated process time and dilution time. However, the uncertainty in calculated OH is probably no more than 50% as indicated by the small difference between our value and the average value 1.5×10^6 cm^{-3} by *Davis et al.* [this issue].

An important consideration in the above discussion is that the travel time from land is defined to be the time between the point of observation and the point where the back trajectory first reaches land. It does not take into account the entrainment of continental boundary layer trace gases

into the free troposphere at points upwind of the landfall point. Since most of the transport from the boundary layer to the free troposphere is due to convective processes [*Gidel*, 1983], which tend to be episodic and scattered, the entrainment may occur far upwind of the landfall point. Obviously, it is possible for this effect to account for a large part of the difference between the process time and the travel time from land calculated above. A key question now is, after taking out the upwind effect, how much of the difference is due to dilution. Unfortunately, we do not have enough information on the time and location of convective events over land during PEM-West to estimate this effect.

7. Discussion

The preceding comparisons of the trajectory, lidar, and atmospheric processing schemes for classifying air masses indicate that the atmospheric processing scheme gives a meaningful relative scale that can be used in conjunction with the other two schemes. More importantly, combining the results of the three schemes (i.e., Figures 7 and 8) with results from a regional model [*McKeen et al.*, this issue] may shed some light on the questions raised in the preceding sections with regard to the role of dilution and the overall consistency between the various schemes over the model domain that covers from 2 to 8 km over eastern China and the western Pacific from 15°N to 50°N and from 100°E to 150°E.

McKeen et al.'s results indicate that the largest model-calculated value of C_2H_2/CO (~2.6; see Figure 9), which is in good agreement with observations made in the model domain, is smaller than the observed values in the free tropospheric air masses classified as continental (C_2H_2/CO > 3.5). Since the model domain contains eastern Asia and uses measured source values of C_2H_2/CO representative of the region (~8.7, *Blake et al.* [this issue]), it is reasonable to conclude that this difference could be due to emissions upwind of eastern Asia. During the period studied, the upwind region was central and western Asia and Europe as the prevailing wind in the free troposphere was mostly westerlies near the western boundary of the model domain. Of course, the effects of boundaries can contribute significantly near areas where the wind is inward from the boundary. In fact, significant amounts of the continental boundary layer tracer species that were observed in the upper troposphere during PEM-WA could owe their origins to regions far upwind of eastern Asia.

When we take the above discussion into account, we find evidence that the difference in calculated process times between two different air masses becomes more comparable to the differences between their travel times from land. For example, the difference in median process time between southern continental less than 2-day air masses (I) and southern continental 2- to 4-day air masses (i) is about 10 days; and the difference in median process time between northern continental less than 2-day air masses (C) and northern continental 2- to 4-day air masses (c) is only about 4 days. Both have relatively large uncertainties compared to the process times starting from emissions because there is large variance in the C_2H_2/CO values of (C) and (I) air masses. The difference in process time value of 4 days between (C) and (c) is only about 2 times the travel time from land; that is, the latter is about equal to the dilution time. In this case, photochemical reactions during the travel time from land contribute approximately as much as dilution to the trends in Figures 7a-7d. Similar arguments can be made for other pairs of air mass types.

To answer the more general question of the dilution time's contribution to the process time, we can first examine points near the model's largest C_2H_2/CO value (~2.6) which most likely come from land areas that are relatively close to the points of observation. In other words, the travel times for these points from land should be relatively short. From Figure 7b they can be deduced to be less than 2 days, which is in agreement with the model estimate. The corresponding process time for points with C_2H_2/CO of 2.6 is about 15 days. This means that dilution can contribute the equivalent of up to 13 days to the process time. Furthermore, since the model's largest (C_2H_2/CO ~2.6) values have a short travel time, the dilution must be primarily due to the entrainment of ambient air during the vertical transport of near-surface trace species to the free troposphere and for compounds with moderate to long lifetimes (>2 days). Photochemistry and horizontal transport processes contribute to the process time at a later stage.

These results clearly indicate that (1) dilution or atmospheric mixing play a controlling role in determining the value of C_2H_2/CO; (2) trends of trace species relative to C_2H_2/CO, such as those displayed in Figures 7a-7h, are primarily controlled by atmospheric mixing; and (3) for compounds less reactive than C_6H_6, photochemical reactions during the travel time from land contribute only a minor part to the trends. Nevertheless, it is important to recall the point made earlier, i.e., "although atmospheric mixing itself is purely a physical process, the rate of dilution is proportional to the photochemical sink because mixing ratios of hydrocarbons in the background air are inversely proportional to their sinks." Without the sinks, atmospheric mixing would not yield any trend. Thus through atmospheric mixing, photochemical reactions do play a controlling role in determining the trends after all. Although this statement appears to contradict statement 3 above, this is not so because the term "reactions" here refers to those operative in the background air over its collective time history before the time of observations, whereas the term "reactions" cited in the earlier statement refers to those operative only along

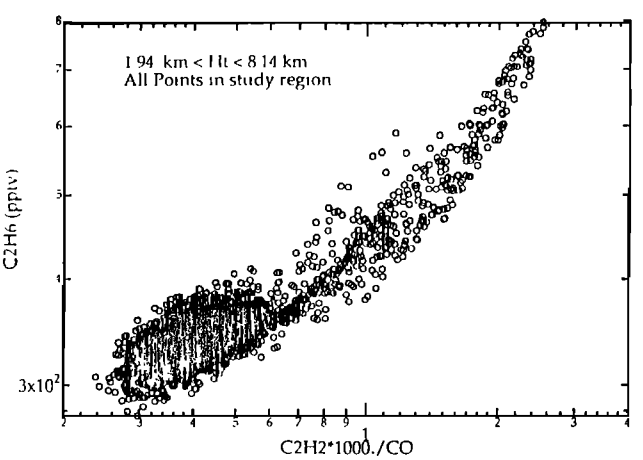

Figure 9. Model-calculated mixing ratio of C_2H_6 versus the ratio C_2H_2/CO between 1.94 km and 8.14 km.

the air mass trajectory between the time of emission and the time of observations.

The answer to why the atmospheric dilution is so dominant in the degree of atmospheric processing when the process time is calculated starting from emissions but not when the difference in process time is calculated between two types of air masses probably lies in the vertical mixing process. After trace species are emitted into the surface layer over land, they are transported vertically by turbulent mixing and convection, sometimes into the free troposphere. These vertical mixing processes tend to be accompanied by entrainment of a large quantity of ambient air which may contain a significant amount of background air. As a result, there is substantial dilution during vertical mixing. After the trace species are transported into the free troposphere by vertical mixing, they are then usually transported horizontally by prevailing winds, which tend to be steady with comparatively little turbulence and hence far less dilution. Therefore the answer to the question is that most of the dilution occurs during the vertical mixing early after emission.

The above comparisons can also be used to obtain valuable information on the sources and sinks for a number of key species. Relatively straightforward conclusions can be drawn from Figures 7a-7d with regard to the sources and sinks of CH_4 and three nonmethane hydrocarbons (NMHC). Their consistent trends relative to C_2H_2/CO suggest the following: (1) major sources of CH_4 and the three NMHCs are located in the continental boundary layer (including the Pacific rim); (2) major sinks of these species are due to OH reactions; and (3) there is no significant oceanic source for these species. We have also made the same type of plots (not shown) for CO, C_2H_2, CFCs, HCFCs, other NMHCs, and a number of model parameters (e.g., O_3 production and destruction rates). No major surprise is found except for CH_3CCl_3 which shows little trend relative to C_2H_2/CO (r^2 = 0.1 for 2-7 km; r^2 = 0.02 for >7 km). Since the lifetime of CH_3CCl_3 against OH reaction is shorter than CH_4, which does exhibit a clear relationship relative to C_2H_2/CO, its (CH_3CCl_3) lack of a trend must be due to a relatively small source in Asia compared to sources in other parts of the northern hemisphere. For CO_2, Figure 7e reveals little additional information than what is already discussed in the previous section, except there is an interesting indication of slightly smaller mixing ratios for air masses at lower latitudes, suggesting a greater continental biogenic sink there.

Two features of O_3 in Figure 7h are worth noting: one is the low mixing ratios in the tropical south marine air masses (S); the other is the high values in fresh continental air masses (C and I). Low O_3 mixing ratios in the tropical Pacific have been well documented to be due to low photochemical production and large photochemical sink [e.g., *Liu et al.*, 1983; *Piotrowicz et al.*,1986]. The high O_3 values in fresh continental air masses are consistent with the fact that there is significant O_3 production in the continental boundary layer due to anthropogenic emissions of O_3 precursors. However, stratospheric intrusion may also contribute significantly to O_3 in continental air masses as indicated by results from a three-dimensional model calculation that show high values of potential vorticities and thus, O_3 over the continent, particularly in the upper troposphere [*Liu et al.*, this issue].

We also find that the modeled gross photochemical O_3 production rates vary as a function of the degree these air masses have been atmospherically processed with average rates ranging from approximately 0.5 ppbv/d at smaller C_2H_2/CO values (~0.3 to 0.4 ppt/ppbv) and increase with increasing values of C_2H_2/CO to an average of approximately 8 ppbv/d at the largest C_2H_2/CO values (~2.5 to 3.5 pptv/ppbv; see Figure 10a). Little altitude dependence is exhibited in the gross production rate when it is expressed in units of parts per billion volts per day (see also discussion by *Davis et al.* [this issue]). As might be expected, since it basically depends on water vapor [see *Davis et al.*, this issue], gross O_3 photochemical loss rates exhibit a nearly independent relationship with C_2H_2/CO values with values averaging approximately 0.5 ppb/d in the greater than 7-km regime and approximately 3 times that rate in the lower (2- to 7-km) altitude regime. This combination results in little correlation of net photochemical tendency (i.e., production rate minus loss rate) with respect to C_2H_2/CO values in the lower-altitude range, where photochemical loss dominates (average net value of approximately -1 ppb/d), and a surprisingly almost linear increase in a resultant net production of O_3 in the upper altitude regime, which increases from approximately +0.2 ppbv/d at the smallest C_2H_2/CO values to approximately +1.5 ppbv/d at the largest. In addition, gross O_3 production rates are, as might be expected, largest in the chemically "youngest" (i.e., continental) air masses (C and I) and smallest in the equatorial marine air masses (S) (see Figure 10b).

Most of the trend in gross O_3 production discussed above is directly related to the observed trend in the precursor NO [*Davis et al.*, this issue], which has the major features of Figure 7g that are different from those of NMHCs. This is consistent with our current understanding that the sources and sinks of reactive nitrogen NO_x (and NO_y) are quite different from those of NMHCs. An efficient heterogeneous removal of NO_y seems to be suggested by the large difference in NO_y mixing ratios between the northern continental less than 2-day (C) and 2- to 4-day (c) air masses. This is also true for the southern continental less than 2-day (I) and 2- to 4-day (i) air masses. However, as discussed earlier, the slope of NO_y between C_2H_2/CO values of 0.5 to 1.5 pptv/ppbv seems too small for air masses that are more atmospherically processed than the northern or southern continental ones (C, c, I, or i), especially if NO_y has a relatively short lifetime (e.g., several days) from heterogeneous removal processes. While part of this trend might be explained by the increases in relatively inert measured NO_y compounds such as HCN as discussed earlier, it cannot explain the exceptionally small slope for NO, especially when a lower and middle tropospheric lifetime against reaction with OH of about 2 days is predicted. Obviously, a noncontinental source(s) of NO is suggested. This is also suggested by the lack of expected trends in NO (and NO_y) values relative to C_2H_2/CO among the various air mass types (Figure 7g). For example, between the northern continental less than 2 days (C) and the northern marine greater than 10 days (N) types of air masses, NO mixing ratios decrease only by about 50% (from about 60 pptv to about 35 pptv). This change for what should be a very short lived compound can be compared to the corresponding decreases of about 35%, 65%, 50%, and 50%, respectively, for C_2H_6, C_3H_8, C_6H_6, and C_2H_2/CO that all have much greater atmospheric

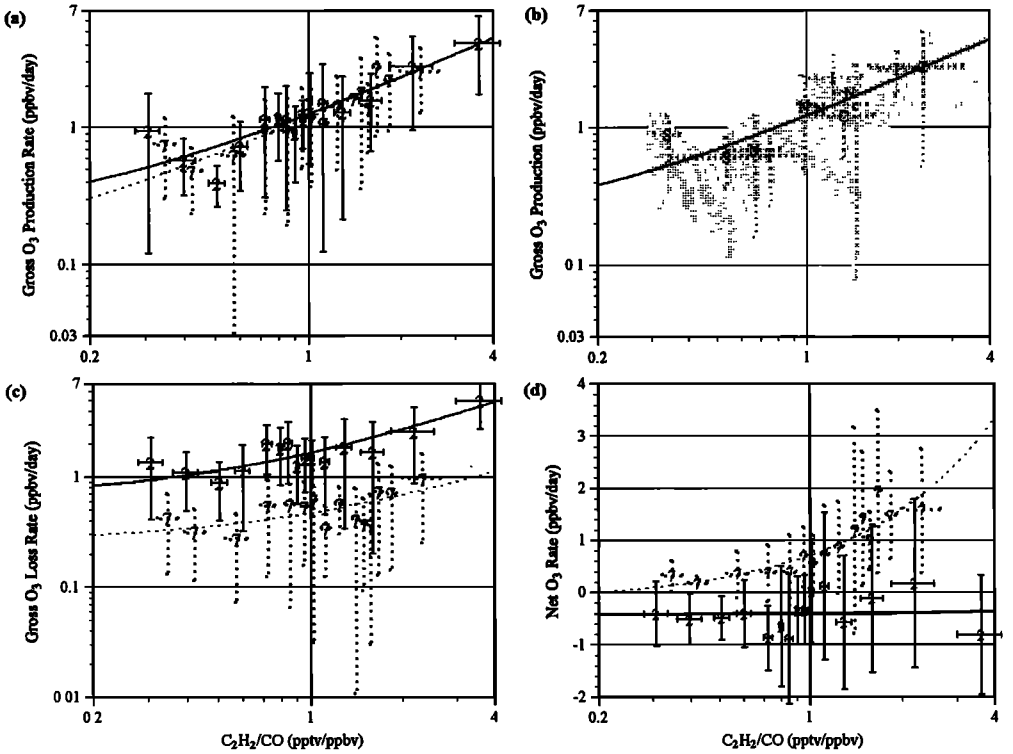

Figure 10. (a) Model-predicted NO_x loss rates as a function of the C_2H_2/CO ratio and (b) measured PAN mixing ratios as a function of C_2H_2/CO ratios, where both show results for two altitude regimes, 2 = 2 to 7 km and 7 = greater than 7 km.

lifetimes. In fact, the model-estimated photochemical NO_x loss rate (*Davis et al.* [this issue] and GTE archive) exhibits a significant increase with increasing values of C_2H_2/CO, going from approximately 5pptv/d to 50pptv/d over the C_2H_2/CO range from 0.3 to 3 pptv/ppbv (see Figure 11a). On average, this loss rate is also nearly independent of altitude when expressed in terms of a mixing ratio (i.e., the differences in absolute rates nearly offset by differences in number density between the two altitude regimes). These daily loss rates are also comparable to the magnitude of NO (or NO_y) within these air masses. Thus with the two types of air masses having at least 8 days of difference between their travel times from land, a decrease of merely 50% in NO (or NO_x) can only be explained by having a significant nonsurface source(s).

Possible candidates for the above nonsurface source(s) of NO (and portions of NO_y) are the emissions from lightning and subsonic aircraft, stratospheric intrusions, and in situ reformation from NO_y compounds. Among the three sources, the source strength of lightning is the largest with a range of 3 to 8 Tg (10^{12} g) per year globally (see review by *Borucki and Chameides* [1984]). The global source strengths of subsonic aircraft and stratospheric intrusions are about 0.7 and 0.5 Tg per year, respectively (see review by *Fehsenfeld and Liu* [1993]). For comparison, anthropogenic emissions in the land surface layer over Asia is about 3 Tg per year [*Kato and Akimoto*, 1992]. Thermal decomposition, reactions with OH, and photolysis are known mechanisms for recycling various NO_y compounds that can be produced from surface emissions, such as PAN, HO_2NO_2, and HNO_3, into the more active NO_x form. However, in the upper troposphere these rates of these processes are all too slow to result in a significant in situ source of NO_x [*Davis et al.*, this issue; *Singh et al.*, this issue]. It is clear that among the three nonsurface sources the lightning source should dominate. This may be the case even in the upper troposphere because the lightning source is probably efficiently mixed up to the upper troposphere by convective processes.

Since about 60% of lightning occurs between 20°S and 20°N [*Hameed and Dignon*, 1988], as opposed to subsonic aircraft emissions and stratospheric intrusions having a larger occurrence at midlatitudes, the latitudinal distribution of NO can be used to differentiate the relative importance of the three sources. In Figure 7g the similarity in NO mixing ratios between northern (c) and southern (I) continental less than 2-day types of air masses also suggests that lightning is important in maintaining relatively high levels of NO in the latter air masses. This point is further supported by the complete lack of an altitude gradient in PAN mixing ratios when expressed against the C_2H_2/CO ordinate (see Figure 11b). In addition, this view is also supported by comparisons of the lidar-based and chemically based schemes. Both the continental convective outflow (C) and the marine convective outflow (O) show enhanced NO levels relative to NMHCs (Figure 8). Specifically, the average ratio of NO/C_2H_6 is 0.06 and 0.1 for (C) and (O) types of air mass, respectively. This is higher than the other types of air masses. In fact, the average ratio of NO/C_2H_6 of clean Pacific air (P) is only 0.05 at a similar altitude (near 8 km) to the (O) air masses, suggesting that lightning in convective activities may be a significant source of the NO (or NO_x) in these air masses (see also *Browell et al.*'s [this

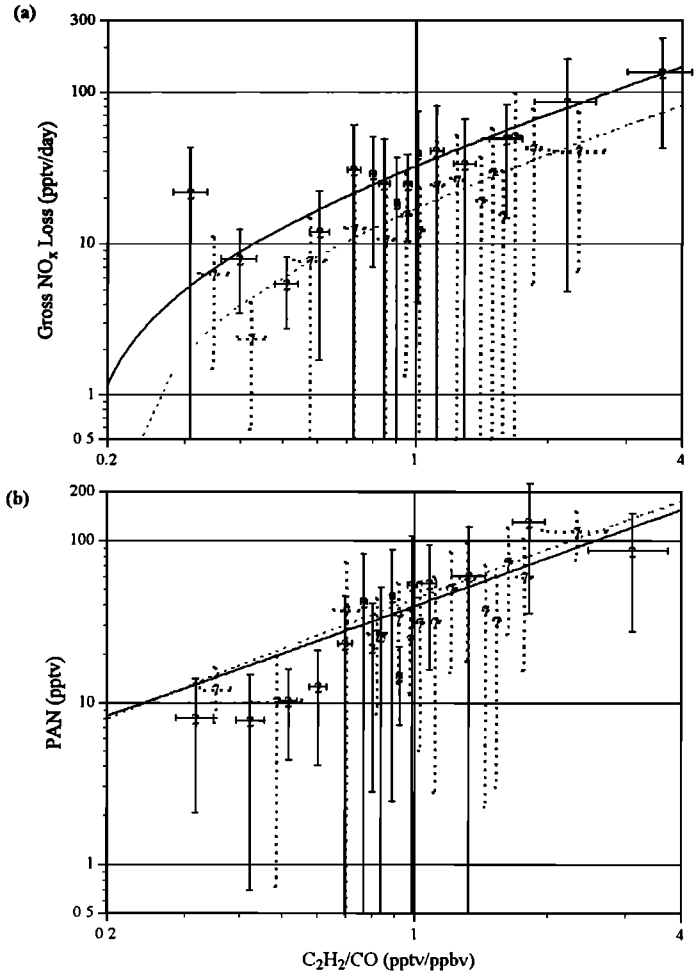

Figure 11. Model-predicted O_3 production and loss rates as a function of the ratio C_2H_2/CO for (a) gross O_3 production in two altitude regimes 2 = 2 to 7 km, 7 = greater than 7 km; (b) same as in Figure 11a showing air masses classified by Gregory et al. and Talbot et al. (see Figure 7); (c) gross O_3 loss in two altitude regimes; and (d) net O_3 photochemical tendency in two altitude regimes.

issue] discussion of the O_3 observations). The ratio of NO_y/C_2H_6 shows similar characteristics as NO/C_2H_6 and similar findings are obtained from inspecting NO relative C_3H_8 [see also *Davis et al.*, this issue], C_6H_6, and other NMHCs. However, the differences between the convective types of air masses and others are not so large, probably due to heterogeneous removal of soluble species of NO_y by clouds and precipitation associated with convective activities.

As for the possibility of a stratospheric source, based on observations made to date in the lower stratosphere (equivalent to the region with 150 pptv < O_3 < 300 ppbv) NO (and NO_x) is a small component of the NO_y budget and is not significantly enhanced relative to O_3 in comparison to upper tropospheric air [e.g., *Murphy et al.*, 1993; *Sandholm et al.*, 1992; *Bradshaw et al.*, 1994]. This would seemingly argue against the lower stratosphere acting as a significant source of the observed NO over the western Pacific, unless an as yet unidentified and efficient mechanism exists that can reconvert stratospheric HNO_3 back into more reactive forms that can yield NO (see also discussion by *Sandholm et al.* [1994]).

The above discussion would seemingly leave only aircraft emissions or some yet unidentified means of recycling HNO_3 as sources competing against lightning as the cause of the observed trends in NO. At first glance the meridional profile of the NO measurements made during PEM-West A does appear to have an upper troposphere NO maximum that corresponds to the latitudes and altitudes that could be expected to have been most heavily impacted by subsonic aircraft emissions from the Pacific rim air traffic corridor (see Figure 12a). However, the occurrence of similar pronounced maximums in the distributions of C_3H_8, C_2H_2, and C_2H_2/CO (Figures 12b-12d) cannot be easily explained by aircraft emissions without orders of magnitudes larger relative enhancements in NO_x and NO_y or extremely fast loss rates resulting in many more 1/e-fold photochemical processing times having elapsed relative to the hydrocarbon compounds since emission. The unlikelihood of either circumstance and the more than casual relationship between all tracers strongly implicates the role of deep convection and further supports either lightning or the recycling of NO_y that was transported vertically in association with deep convection as perhaps the dominant source(s) of NO (and NO_x) to the upper free troposphere during PEM-West A.

The importance of deep convection to the upper troposphere is also implicated by another valuable piece of

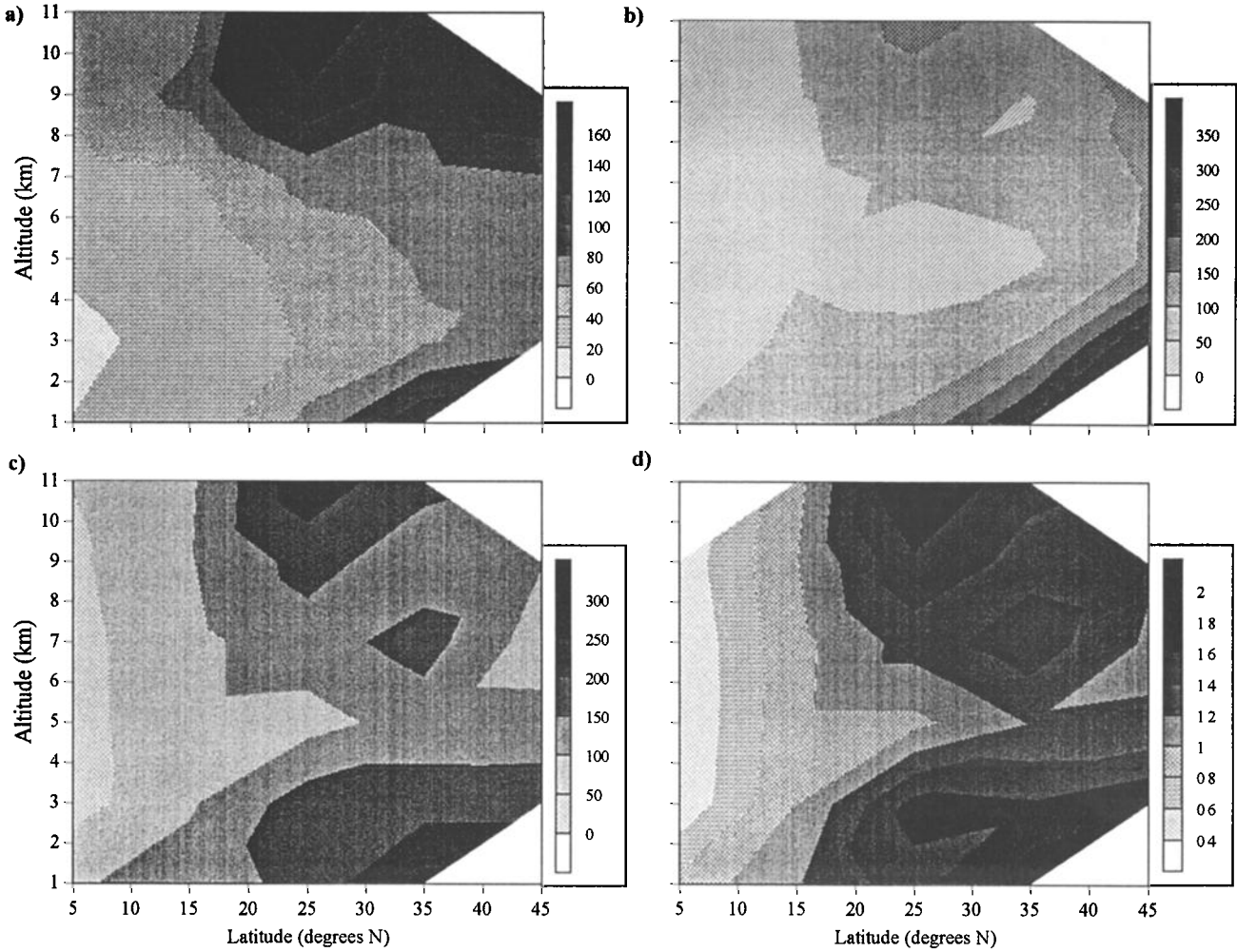

Figure 12. Meridional profile of western Pacific PEM-WA measurements for (a) NO_x ($NO_x = NO + NO_2$), (b) C_3H_8, (c) C_2H_2, and (d) C_2H_2/CO (pptv/ppbv).

information that can be derived by examining the ratio of C_2H_2/CO of the stratospherically influenced air masses (F) defined by the lidar-based scheme. These air masses were located primarily in the middle and upper troposphere and were usually associated with descending air characterized by relatively high ozone (see Figure 8h), low abundances of aerosols, and water vapor. As for continental boundary layer tracer species in these air masses, one would expect a high degree of atmospheric processing. However, observations show that this is not the case, as the C_2H_2/CO values of (F) in Figures 8a-8h are surprisingly high. The median value is about 0.9 pptv/ppbv, which is near the average of all air masses (i.e., nearly half of all air masses, including all southern marine greater than 10 days (S), most of southern continental 2-4 days (i), and about half of northern marine greater than 10-day (N) types, had experienced more atmospheric processing relative to C_2H_2/CO than the stratospherically influenced (F) type of air mass). This suggests that the transport of boundary layer tracer species to the upper troposphere, most likely by convective processes, is highly efficient. Furthermore, it suggests that the photochemical reactions and dilution are relatively slow within the upper troposphere. Once transported to the upper troposphere, the continental boundary layer tracer species become well mixed horizontally due to strong prevailing winds and relatively slow photochemical reactions. This is substantiated by the relatively large concentrations of CH_4, NMHC, CO, and other continental tracers in the (F) type air masses [see also *Gregory et al.*, this issue] and by the altitude distributions of the continental boundary layer tracers where significant differences in mixing ratios were found between continental air and marine air below 9 km but not above 9 km [*Gregory et al.*, this issue; *Talbot et al.*, this issue; *Liu et al.*, this issue].

The process time corresponding to a median C_2H_2/CO value of 0.9 pptv/ppbv is about 30 days, which is long enough for an air mass with 13 m/s zonal wind speed to circle the whole globe at 30° latitude. Since the average zonal wind speed near 10 km altitude is about 15 m/s at midlatitudes in the fall, it is obvious that the continental boundary layer trace gases, such as the CO and NMHCs observed in the upper troposphere, may originate from regions far upwind of the Asian continent. This is supported by results from a regional scale model calculation that give highly patchy distributions for trace gases transported into the upper troposphere by convective processes from the

boundary layer of eastern Asia [*Liu et al.*, this issue]. The relatively uniform distribution of continental boundary layer tracer species observed in the upper troposphere requires that they have origins far upwind of eastern Asia. In fact, the upper troposphere over the western Pacific observed during PEM-West A may contain a significant contribution from air masses transported by convective processes from the boundary layer of all land areas in the northern hemisphere.

The above finding on the transport of continental trace species to the upper troposphere is extremely valuable for testing the vertical transport parameterization used in models. The relative values of continental boundary layer tracers such as NMHCs in the stratospherically influenced air masses can be used to evaluate quantitatively the vertical transport schemes of models which usually are highly parameterized and difficult to evaluate for their accuracy. Many important tropospheric issues cannot be adequately addressed until vertical transport processes are accurately simulated in models. For example, tropospheric ozone budget depends critically on the vertical transport of NO_x from the continental boundary layer to the free troposphere [*Liu et al.*, 1987; *Pickering et al.*, 1990; *Jacob et al.*, 1993]. Another example is the transport of sulfur species and aerosols to the free troposphere which are important to the radiation budget.

8. Summary

We have employed a chemically based air mass classification scheme using the combustion products C_2H_2 and CO as tracers of continental source emissions. For the data taken during the 1991 PEM-West A program, the degree of atmospheric processing that reflects the combined effects of chemistry and mixing appears to be well represented by the measured ratio C_2H_2/CO. A large number of compounds having free tropospheric photochemical lifetimes from days (e.g., NO_x and C_6H_6) to years (CH_4) were found to display similar tendencies with respect to the degree of atmospheric processing indicated by the ratio C_2H_2/CO.

Comparison of the C_2H_2/CO-based atmospheric processing scheme with two other independent schemes, i.e., isentropic back-trajectory-based scheme and lidar O_3 and aerosol-based scheme, for classifying air masses indicates that the C_2H_2/CO-based scheme is successful in providing a consistent and meaningful measure of the degree of atmospheric processing for the majority of the air masses classified by the latter two schemes. In addition, the C_2H_2/CO-based scheme appears to segregate between the chemical differences in air masses with greater than 10-day travel times from sources and for those modified by convective events. The C_2H_2/CO-based scheme and the trajectory-based scheme are more compatible with each other than with the lidar-based scheme because the former two schemes use the land as their reference point.

The C_2H_2/CO-based scheme also compares very well with results calculated by a three-dimensional regional model except for a shift in the distribution of model points toward smaller values of C_2H_2/CO, which is attributed to the effect of emissions upwind of the model domain. The comparison indicates that most of the initial atmospheric processing following emissions of trace species near the surface is due to entrainment of ambient air during the vertical transport of the trace species from the surface to the free troposphere. Photochemistry and horizontal transport processes contribute to the atmospheric processing at a later stage.

The complimentary nature of these three schemes enable them to be combined in order to obtain valuable information on the sources and sinks for a number of key species. First, a significant noncontinental source(s) of NO (and NO_x) in the free troposphere is indicated and is attributed to either the emissions from lightning or the recycling of NO_y transported through deep convection. Second, for the western Pacific, continental boundary layer tracer species, such as hydrocarbons, are vertically transported into the upper troposphere as efficiently as they are transported into the midtroposphere. Third, the CO and NMHCs observed in the upper troposphere may reflect a significant contribution from convectively transported surface emissions from northern hemispheric land areas other than Asia. Finally, we believe that results of the C_2H_2/CO-based scheme can be extremely valuable for the quantitative evaluation of the vertical transport processes that are usually parameterized in models.

Acknowledgments. The authors would like to thank the NASA Ames DC-8 flight and ground crews for their work during PEM-WA. Our special thanks go to our Asian and U.S. base hosts and to Jim Hoell, Richard Bendura, and Jaqueline Johnson for coordinating all of our logistics needs. We would like to also acknowledge the contributions of Sandra Farber, Nicole Shumaker, and Christy Robb toward the preparation of this manuscript and to one of the anonymous reviewers for his/her effort in providing excellent recommendations for revision of this manuscript. This research was supported in part by the National Oceanic and Atmospheric Administration's Climate and Global Change Program's Atmospheric Chemistry Project and by the National Aeronautics and Space Administration's Tropospheric Chemistry Program.

References

Altschuller, A. P., The production of carbon monoxide by the homogeneous NO_x-induced photooxidation of volatile organic compounds in the troposphere, *J. Atmos. Chem.*, 13, 155-182, 1991.

Bachmeier, A. S., R. E. Newell, M. C. Shipham, Y. Zhu, D. R. Blake, and E. V. Browell, PEM-West A: Meteorological Overview, *J. Geophys. Res.*, this issue.

Blake, D. R., T.-Y. Chen, T. W. Smith Jr., C. J.-L. Wang, O. W. Wingenter, N. J. Blake, F. S. Rowland, and E. W. Mayer, Three-dimensional distributions of nonmethane hydrocarbons and halocarbons over the northwestern Pacific during the 1991 Pacific Exploratory Mission (PEM-West A), *J. Geophys. Res.*, this issue.

Borucki, W. J., and W. L. Chameides, Lightning: Estimates of the rates of energy dissipation and nitrogen fixation, *Rev. Geophys.*, *22*, 363-372, 1984.

Browell, E. V., et al., Large-scale air mass characteristics observed over western Pacific during summertime, *J. Geophys. Res.*, this issue.

Collins, J. E., G. W. Sachse, B. E. Anderson, R. C. Harriss, S. Sandholm, L. O. Wade, L. G. Buracy, and G. F. Hill, Airborne nitrous oxide observations over the western Pacific Ocean: September-October 1991, *J. Geophys. Res.*, this issue.

Crawford, J., et al., Photostationary state analysis of the NO_2-NO system based on airborne observations from the western and central North Pacific, *J. Geophys. Res.*, this issue.

Davis, D. D., et al., Assessment of ozone photochemistry in the western North Pacific as inferred from PEM-West A observations during fall 1991, *J. Geophys. Res.*, this issue.

DeMore, W. B., S. P. Sander, M. J. Molina, D. M. Golden, R. F. Hampson, M. J. Kurylo, C. J. Howard, and A. R. Ravishankara, Chemical kinetics and photochemical data for use in stratospheric modeling, in *Evaluation 10, JPL Publ. 90-91*, Jet Propul. Lab., Pasadena, Calif., 1992.

Fehsenfeld, F. C., and S. C. Liu, Tropospheric ozone: Distribution and sources, in *Global Atmospheric Chemical Change*, pp. 169-231, edited by C.N. Hewitt and W. T. Sturges, Elsevier Science, New York, 1993.

Gidel, L. T., Cumulus cloud transport of transient tracers, *J. Geophys. Res., 88,* 6587-6599, 1983.

Gregory, G. L., A. S. Bachmeier, D. R. Blake, B. G. Heikes, D. C. Thornton, J. D. Bradshaw, and Y. Kondo, Chemical signatures of aged Pacific marine air: Mixed layer and free troposphere as measured during PEM-West A, *J. Geophys. Res.*, this issue.

Hameed, S., and J. Dignon, Changes in the geographical distributions of global emissions of NO_x and SO_2 from fossil fuel combustion between 1966 and 1980, *Atmos. Environ.*, *22*, 441-449, 1988.

Hoell, J. M., Jr., D. D. Davis, S. C. Liu, R. Newell, M. Shipham, H. Akimoto, J. McNeal, R. J. Bendura, and J. W. Drewry, Pacific Exploratory Mission - West A (PEM-West A), *J. Geophys. Res.*, this issue.

Hübler, G., et al., Total reactive oxidized nitrogen (NO_y) in the remote Pacific troposphere and its correlation with O_3 and CO: Mauna Loa Observatory, *J. Geophys. Res., 97,* 10,427-10,447, 1992.

Jacob, D., J. Logan, G. Gardner, R. Yevich, C. Spivakovsky, S. Wofsy, S. Sillman, and M. Prather, Factors regulating ozone over the United States and its export to the global atmosphere, *J. Geophys. Res, 98,* 14,817-14,826, 1993.

Kato, N., and H. Akimoto, Anthropogenic emissions of SO_2 and NO_x in Asia: Emission inventories, *Atmos. Environ., 26A,* 2997-3017, 1992.

Liu, S. C., M. McFarland, D. Kley, O. Dafiriou, and B. Huebert, Tropospheric NO_x and O_3 budget in the equatorial Pacific, *J. Geophys. Res, 88,* 1360-1368, 1983.

Liu, S. C., M. Trainer, F. C. Fehsenfeld, D. D. Parrish, E. J. Williams, D. W. Fahey, G. Hübler, and P. C. Murphy, Ozone production in the rural troposphere and the implications for regional and global ozone distributions, *J. Geophys. Res., 92,* 4191-4207, 1987.

Liu S. C., et al., Model study of tropospheric trace species distributions during PEM-West A, *J. Geophys. Res.*, this issue.

Lovelock, J. E., *Anal. Chem., 33,* 162, 1961.

McKeen, S. A., and S. C. Liu, Hydrocarbon ratios and photochemical history of air masses, *Geophys. Res. Lett., 20,* 2363-2366, 1993.

McKeen, S., S. C. Liu, E.-Y. Hsie, X. Lin, J. Bradshaw, S. Smyth, G. L. Gregory, and D. R. Blake, Hydrocarbon ratios during PEM-West A: A model perspective, *J. Geophys. Res.*, this issue.

Merrill, J. T., Trajectory results and interpretation for PEM-West A, *J. Geophys. Res.*, this issue.

Murphy, D. M., D. W. Fahey, M. H. Proffitt, S. C. Liu, D. R. Chan, C. S. Eubank, S. R. Kawa, and K. K. Kelly, Reactive nitrogen and its correlation with ozone in the lower stratosphere and upper troposphere, *J. Geophys. Res., 98,* 8751-8774, 1993.

Parrish, D.D., C.J. Hahn, E.J. Williams, R.B. Norton, F.C. Fehsenfeld, H.B Singh, J.D. Shetter, B.W. Gandrud, and B.A. Ridley, Indications of photochemical histories of pacific air masses from measurements of atmospheric trace species at Point Arena, California, *J. Geophys. Res., 97,* 15,883-15,901, 1992.

Pickering, D. E. , A. M. Thompson, R. R. Dickerson, W. T. Luke, D. P. McNamara, J. P. Greenberg, and P. R. Zimmerman, Model calculations of ozone production potential following observed convective events, *J. Geophys. Res., 95,* 14,049-14,062, 1990.

Piotrowicz, S. R., D. A. Boren, and C. J. Fischer, Ozone in the boundary layer of the equatorial Pacific Ocean, *J. Geophys. Res., 91,* 13,113-13,120, 1986.

Sandholm, S. T., et al., Summertime tropospheric observations related to N_xO_y distributions and partitioning over Alaska: Arctic Boundary Layer Expedition 3A, *J. Geophys. Res., 97,* 16,481-16,509, 1992.

Sandholm, S. T., et al., Summertime partitioning and budget of NO_y compounds in the troposphere over Alaska and Canada: ABLE 3B, *J. Geophys. Res., 99,* 1837, 1994.

Singh, H. B., and P. B. Zimmerman, Atmospheric distribution and sources of nonmethane hydrocarbons, in *Gaseous Pollutants: Characterization and Cycling*, John Wiley, New York, 1992.

Talbot, R., et al., Chemical characteristics of continental outflow from Asia to the troposphere over the western Pacific Ocean during September-October 1991: Results from PEM-West A, *J. Geophys. Res.*, this issue.

J. Bradshaw (corresponding author), D. Davis, S. Sandholm, and S. Smyth, School of Earth and Atmospheric Sciences, Georgia Institute of Technology, Atlanta 30332-0340.

S. Liu and S. McKeen, Aeronomy Laboratory, NOAA, Boulder, Colorado 80303

B. Anderson, E. Browell, J. Collins, G. Gregory, and G. Sachse, NASA Langley Research Center, Hampton, Virginia 23665-5225.

R. Talbot, Institute for the Study of Earth, Oceans, and Space, University of New Hampshire, Durham 03824.

D. Blake and S. Rowland, Department of Chemistry, University of California at Irvine, Irvine, California 92717.

M. Fenn, Science Applications International Corporation, Hampton, Virginia 23681.

J. Merrill, Center for Atmospheric Chemistry Studies, Graduate School of Oceanography, University of Rhode Island, Narragansett, Rhode Island 02882.

S. Bachmeier, Lockheed Engineering and Sciences Company, Hampton, Virginia 23681.

D. Thornton, Department of Chemistry, Drexel University, Philadelphia, Pennsylvania 19104.

H. Singh, NASA Ames Research Center, Moffett Field, California 94035.

(Received May 9, 1994; revised March 21, 1995; accepted May 25, 1995.)